MYF6-Mediated Muscle-Bone Cross-Talk and its Effect on Bone Remodelling

Nabila Karam

Department of Human Genetics, McGill University, Montreal

August 2020

A thesis submitted to McGill University in partial fulfilment of the requirements of the degree

of Master of Science

I am very humbly, dedicating this thesis to my mother, Laila Chenguiti and my husband, Mohammad Sadegh Rahbary.

Abstract

Beside its ability to provide force and generate energy, the skeletal muscle is also an endocrine organ that affects the peripheral organs and tissues in ways that explain the beneficial effects of physical activity. Upon contraction, myokines (which are cytokines and peptides originating from the muscle) are produced and released into the bloodstream. Myokines target a vast array of receptors on different tissues and organs to ensure a coherent communication and adaptation between various parts of the body. It has been recently discovered that MYF6, one the four myogenic regulatory factors, is behind the expression of some of these myokines. MYF6 is the principal myogenic regulatory factor (MRF) that is consistently expressed in the mature myofibers. A *Myf6* knock-out mouse model has been successfully generated. These mice have a smaller pool of muscle stem cells, also called satellite cells, compared to their wild-type counterparts. But more importantly, these mice have significantly reduced levels of circulating myokines, both in the secretome of their muscle fibers and their blood serum. Some of these validated myokines are VEGF-a and EGF. We hypothesised that such significant reduction in circulating myokine levels may affect the development of the bones. Muscle and bones are notable for their continuous myokines and osteokines cross-talk. For that reason, assessing the overall health of the *Myf6*-KO long bones was the logical next step. Since myokines expression is up-regulated following exercise, *Myf6*-KO mice and controls were subjected to an endurance swimming test. Swimming allows muscles to move while maintaining a minimal impact on the bones, which is ideal to avoid the confounding effects of exercise in this context. Here we show that, overall, the MYF6-related loss of myokines has no significant effect on the bones' structural and mechanistic properties.

Résumé

Outre sa capacité à fournir de la force physique et à générer de l'énergie, le muscle s'est également adapté pour être un organe endocrinien qui affecte les organes et les tissus périphériques de manière à expliquer les effets bénéfiques de l'activité physique. Lors de la contraction des muscles, les myokines (qui sont des cytokines et des peptides provenant du muscle) sont produites et libérées dans la circulation sanguine. Les myokines ciblent une vaste gamme de récepteurs sur différents tissus et organes pour assurer une communication et une adaptation cohérentes et optimales entre les différentes parties du corps. Il a été récemment découvert que MYF6, l'un des quatre facteurs régulateurs myogéniques, est à l'origine de l'expression de certaines de ces myokines. MYF6 est le seul facteur de régulation myogénique (FRM) qui est systématiquement produit dans les fibres matures du muscle. Un modèle de souris MYF6 a été généré avec succès. Ces souris ont un réservoir de cellules souches musculaires, également appelées cellules satellites, qui est réduit de manière significative par rapport à leurs homologues de type sauvage. Mais plus important encore, ces souris ont des niveaux de myokines circulants considérablement réduits, tant dans le sécrétome de leurs fibres musculaires que dans leur sérum sanguin. Certaines de ces myokines qui ont été validées sont VEGF-a et EGF. Nous avons émis l'hypothèse qu'une telle réduction significative des niveaux de myokines qui circulent dans le sang pourrait affecter le développement des os. Les muscles et les os sont connus pour leur diaphonie continue qui se fait par le biais des myokines et des ostéokines. Pour cette raison, l'évaluation de la santé globale des os longitudinaux chez les souris *Myf6*-KO était la prochaine étape logique. Étant donné que l'expression des myokines est régulée à la hausse suite à l'activité physique, les souris témoins et les souris *Myf6*-KO ont été soumises à un test de natation d'endurance. La natation permet aux muscles de se contracter tout en conservant un impact minimal sur les os, ce qui est idéal pour éviter les effets de confusion de l'exercice dans ce contexte-ci. Ici, nous montrons que, globalement, la perte de myokines liée à MYF6 n'a pas d'effet significatif sur les propriétés structurales et mécaniques des os.

Table of Contents

List of Abbreviations

MRF : myogenic regulatory factor

Myf6 : Myogenic factor 6

MyoD : Myoblast determination protein

Pax7 : Paired box 7

Pax3: Paired box 3

MuSCs: muscle stem cells

SCs: satellite cells

IL-6: Interleukin 6

IL-15 : Interleukin 15

LIF: Leukemia inhibitory factor

OSM: Oncostatin M

VEGF-a: Vascular endothelial growth factor a

EGF: Epidermal growth factor

Myf6-KO: *Myf6* knock-out

WT: wild-type

Het: heterozygous

microCT: microcomputed tomography

SR-CT: synchrotron radiation microtomography

FACS: fluorescence-activated cell sorting

BV/TV: bone volume fraction

T.Ar: total crossectional tissue area

Ct.Ar: cortical area

Ma.Ar: medullary area

Ps.Pm: periosteal tissue perimeter

Ec.Pm: endosteal (endocortical) perimeter

Ct.Th: cortical thickness

Imax: maximum moment of inertia

Imin: minimum moment of inertia

Tb.Sp: trabecular separation

Tb.Th : trabecular thickness

VOI: volume of interest

ROI: region of interest

TRAP: tartrate-resistant acid phosphatase

CTXII: C-telopeptide fragments of type II collagen

PINP: pro-collagen I N-terminal propeptide

List of Figures

Acknowledgments

This work would not have been possible without the support of many people, starting with my supervisor, Dr. Vahab Soleimani. Dr. Vahab Soleimani believed in me and gave me all the resources I could have possibly needed. He supported me through every step, without ever failing me or any of my colleagues through my own, and their journey. He truly is a mentor as opposed to a simple supervisor.

I would like to also thank my supervisory committee members, Dr. Bettina Willie and Dr. René Saint-Arnaud, for their continued guidance and support. They put many resources at my disposition and carefully listened to my needs throughout this academic journey.

I would like to thank all of my past and current colleagues for training me, assisting me during some time-consuming experiments, and especially providing me with emotional support when I needed it the most. My graduate life would have been different without them.

And finally, I would like to thank my mother and my husband for caring about me the way they did. Their support was beyond everything I could have ever imagined. They created an environment in which I could thrive and feel free to explore my potential. They believed in me more than I ever believed in myself.

I, Nabila Karam, hereby declare that I am the sole contributor to the chapters and figures shown in the main body of this thesis. Figures S1 to S3 in the appendix were extracted from this manuscript:

Myf6/MRF4 is a Myogenic Niche Regulator Required for the Maintenance of the Muscle Stem Cell Pool

Felicia Lazure, Darren M. Blackburn, **Nabila Karam**, Korin Sahinyan, Ahmad Sharanek,

Duy Nguyen, Aldo H. Corchado, Christoph Lepper, Hamed S. Najafabadi, Theodore J. Perkins, Arezu Jahani-Asl, Vahab Soleimani.

bioRxiv 691386; doi: https://doi.org/10.1101/691386

And are used here with the permission of Dr. Vahab Soleimani and the first co-authors, Felicia Lazure and Darren M. Blackburn.

Chapter 1: Introduction

1.1- Skeletal muscle structure and function

In vertebrates, skeletal muscle is derived from the somites (Le Grand and Rudnicki 2007). As the somites mature, myogenic progenitor cells become more defined in terms of their molecular signature and their spatial location within the developing organism (Baghdadi and Tajbakhsh 2018) - and eventually, they give rise to the mature muscle.

Skeletal muscle is a subtype of striated muscle, beside the cardiac muscle (Mukund and Subramaniam 2020). Skeletal muscle differentiates itself from cardiac muscle mainly by its ability to exhibit fatigue and generate voluntary movement (Gillies and Lieber 2011). Skeletal muscle is highly innervated and vascularized to support its energy needs (Zurlo, Larson et al. 1990).

The composition and structure of mature muscle is complex and highly organized. At maturity, skeletal muscle represents between 30% to 40% of the body mass in both mice and humans (Baghdadi and Tajbakhsh 2018). The sarcomere is the basic cellular unit of skeletal muscle (Gillies and Lieber 2011). Many sarcomeres can be found along one myofibril. Many myofibrils can be found within a myofiber, which is surrounded by the sarcolemma. Many myofibers form a fascicle and are surrounded by the endomysium. Many fascicles are surrounded by the perimysium and are confined within the epimysium (Gillies and Lieber 2011). The epimysium is hence the outside layer that can be seen on the gross muscle, which is linked to the tendons (Gillies and Lieber 2011). Motor neurons and blood vessels (and associated capillaries) can be found throughout these structures (Gillies and Lieber 2011). Such organization allows for the generation of contraction, more articulated movement (Slater 2017), and more effective energy production (Wannamethee, Shaper et al. 2000). Indeed, not only is skeletal muscle equipped with many mitochondria that support its high energy requirements (Mukund and Subramaniam 2020) but it also evolved to incorporate different isoforms of myofibers that can support a specific type of exercise rather than another (Neunhäuserer, Zebedin et al. 2011). For these reasons, skeletal muscle is considered highly plastic throughout one's life. Skeletal muscle physiological and anatomical properties such as mass and overall metabolism can change dramatically following physical activity, lack of activity, or hormonal change (Baldwin and Haddad 2019).

1.2- Muscle as an endocrine organ

In addition to its ability to produce movement and energy, a less known function of the skeletal muscle has been discovered two decades ago. It has been shown that the skeletal muscle has adapted to be an endocrine organ as well (Febbraio and Pedersen 2002), just like it was hypothesized four decades earlier (Goldstein 1961). As we move and exercise, humoral factors (cytokines and peptides) are produced by the muscle, released into the bloodstream, and detected by other organs where they activate or repress diverse pathways (Febbraio and Pedersen 2002) (Pedersen and Febbraio 2008). These pathways are not all necessarily related to the contractile functions or the homeostasis of the muscle itself but rather span a vast array of bodily functions (Pedersen and Febbraio 2008). These peptides and cytokines were eventually baptized 'Myokines' after being called 'work factors', 'work stimulus', and 'humoral factors' at first (Pedersen and Febbraio 2008) (Pedersen, Steensberg et al. 2003) (Keller, Steensberg et al. 2001).

Myokines have a paracrine, endocrine, or autocrine function. Past observations have shown that as we exercise, peripheral organs seemed to get healthier. This led to the publication of many memos by national health agencies and organizations in the late 1990's (1997, 1998, 1998, 1998). Many studies proved that regular and moderate exercise in one's lifestyle has many beneficial effects on the body, but less was known about the molecular basis of such observations. It was reported that the risk of being affected by chronic diseases such as cardiovascular diseases (Wannamethee, Shaper et al. 2000), type 2 diabetes (Wannamethee, Shaper et al. 2000), Alzheimer's disease (Friedland, Fritsch et al. 2001), and dementia (Verghese, Lipton et al. 2003) is significantly reduced in active individuals when compared to those with a sedentary life style. The discovery of myokines partially answered the questions as to how the body benefits from exercise. To date, between 100 to 300 myokines have been identified and linked to different communicatory pathways and cross-talk between tissues, depending on the definition used (Gorgens, Eckardt et al. 2015). These myokines were identified by either examining the content of the fiber secretome in vitro (Catoire, Mensink et al. 2014) (Bortoluzzi, Scannapieco et al. 2006) or by the analysis the blood of active individuals by selecting the proteins that were elevated post-exercise (He, Tian et al. 2018). Recently, global mRNA sequencing from biopsies taken from active individuals has also been used to target novel myokines that might have a lower protein abundance at a basal state (Pourteymour, Eckardt et al. 2017).

1.3- Myogenic regulatory factors (MRFs) and myogenesis

Skeletal muscle is first formed prenatally (de novo embryonic muscle development) and the process continues postnatally (adult myogenesis)(Bentzinger, Wang et al. 2012) (Kuang, Kuroda et al. 2007) (Asfour, Allouh et al. 2018). Both processes are distinct but share the same myogenic factors that allow for the muscle to be generated from precursor/progenitor cells. These myogenic regulatory factors (MRFs) are: Myogenic Factor 5 (MYF5), Myoblast Determination protein (MYOD), Myogenin (MYOG), and Myogenic Factor 6 (MYF6/MRF4) (Asfour, Allouh et al. 2018). Following a set of well-orchestrated and tightly regulated steps by the MRFs, precursor cells are activated, which eventually give rise to a mature myofiber (Fan, Li et al. 2012).

Prenatally, the MRFs are expressed in the somites, which then evolve to be sclerotome, dermomyotome, myotome (precursor of the segmented muscle) and syndetome (tendon progenitors) (Zammit 2017). Postnatally, the MRFs are mainly expressed in the satellite cells (Scs), as opposed to the somite-derived myogenic progenitor cells (Zammit 2017). Satellite cells, also called muscle stem cells (MuSCs), are quiescent mononucleated cells residing in their niche, between the basal lamina and the sarcolemma of their associated myofiber (Mourikis and Relaix 2016). At birth, satellite cell nuclei make up 30% to 35% of total muscle nuclei but that proportion decreases with time, accounting for less than 5% in adult muscle (Allbrook, Han et al. 1971) (Shefer, Van de Mark et al. 2006) (Bareja and Billin 2013). Satellite cells are mitotically paused cells, arrested at the Go phase with a high expression of the transcriptional factor Paired Box 7(PAX7), Paired Box 3 (PAX3) or both (Relaix, Rocancourt et al. 2005). Some are also $MYF5^{+}$ (around 90% of the $PAX7^{+}$ cells) while a smaller portion is $MYF5^{-}$ (10% or the $PAX7^{+}$ cells) (Kuang, Kuroda et al. 2007). This heterogeneity is the result of an asymmetrical division following activation, that allows for a portion of the daughter cells to return to quiescence (Kuang, Kuroda et al. 2007).

The activity and expression of the MRFs is tightly orchestrated (Zammit 2017). The myogenic differentiation program is contingent to temporal activity and muscle environment (Asfour, Allouh et al. 2018). Upon activation through external stimuli such as injury, intense physical activity, extended use of some anabolic steroid drugs (Asfour, Allouh et al. 2018) (Friedrichs, Wirsdöerfer et al. 2011), satellite cells start decreasing their expression of PAX7,

allowing for the expression of MYOD (Soleimani, Punch et al. 2012) (Seale, Sabourin et al. 2000).

As the myogenic program goes on, the satellite cells leave their quiescent state and start proliferating (Asfour, Allouh et al. 2018). Eventually, Myogenin takes over MYOD (Füchtbauer and Westphal 1992, Du, Jin et al. 2012, Zammit 2017). As the satellite cells differentiate and start fusing, Myogenin is downregulated and is gradually and finally replaced by MYF6 (Asfour, Allouh et al. 2018) (Zammit 2017) (Lazure, Blackburn et al. 2019). MYF6 is the only MRF to be expressed throughout the lifetime of the mature fiber (Lazure, Blackburn et al. 2019).

1.4- Myf6/MRF4

Different MRFs have well-orchestrated functions that can not, in most of them, be compensated by one another (Lazure, Blackburn et al. 2019). Although some have overlapping functions and targets, some retain unique roles that require them to be specifically present for the successful completion of the myogenic program (Lazure, Blackburn et al. 2019) (Haldar, Karan et al. 2008). As previously stated, MYF6/MRF4 is the last myogenic regulatory factor to be expressed in the myogenic program. As opposed to the other MRFs which are transient, MYF6 is highly expressed in mature myofibers (Lazure, Blackburn et al. 2019).

In humans, the *Myf6* gene is located in chromosome 12, only 6.5 Kb upstream the *Myf5* locus (Braun, Bober et al. 1990). Knockout of *Myf6* was initially proven difficult because of its proximity to *Myf5 (*Braun and Arnold 1995) and knockdowns were used instead to investigate the role of MYF6 (Moretti, Ciciliot et al. 2016). A *Myf6* knockout model was later successfully generated; the mice were having life spans comparable to their wild type counterparts (Southard, Low et al. 2014). The *Myf6*-CE mice have a Cre-ERT2 cassette knocked into the first exon of the *Myf6* gene (Southard, Low et al. 2014) (Lazure, Blackburn et al. 2019). Surprisingly, mice with both null alleles for *Myf6* have normal skeletal muscles and cannot be physically distinguished from their wild type littermates (Southard, Low et al. 2014) (Lazure, Blackburn et al. 2019). At three-months of age however, a phenotype can be observed in the *Myf6*-KO mice; their satellite cells pool is significantly reduced compared to the matched wild-type (WT) mice (Lazure, Blackburn et al. 2019). Such

a trend is accentuated with time, with an even larger differences in pool size (Lazure, Blackburn et al. 2019).

More importantly, It was also shown that MYF6 is the master regulator of a vast array of myokines (Lazure, Blackburn et al. 2019). Some of these myokines are directly involved in the maintenance of the satellite cells' niche, which explains their gradual loss. When *Myf6* is knocked-out in the muscle, the mice show no defects in regeneration but have reduced myokine levels in their blood serum following an RNAseq and mirco-array analysis (Lazure, Blackburn et al. 2019). Vascular endothelial growth factor a (VEGF-a), Epidermal Growth Factor (EGF), Interleukin-6 (IL-6), Interleukin 15 (IL-15), Oncostatin M (OSM), Leukemia Inhibitory Factor (LIF) are some of these myokines (Lazure, Blackburn et al. 2019). Motif analysis identified canonical E-box motif and the Mef2a DNA binding motif as the most enriched binding sequences of MYF6, and confirmed some of those targets (Lazure, Blackburn et al. 2019).

Interestingly, not only is MYF6 expression maintained throughout the life of the mature fiber, but it is also upregulated following both aerobic and resistance exercise (Caldow, Thomas et al. 2015, D'Lugos, Patel et al. 2018). This upregulation in MYF6 is accompanied with an upregulation in the myokines that are under its transcriptional regulation (Ciano, Mantellato et al. 2019) (Singh, Carpenter et al. 2016) (Yao, Lafage-Proust et al. 2004). It is possible that a mechanistic stimulus triggers the expression of MYF6, which in turns activates the expression of its associated myokines.

1.5- Bone and muscle crosstalk

Many organs with the appropriate receptors are affected by the circulating myokines. This endocrine function provides the body with an adaptative response and efficient communication between the organs, especially in situations of increased energy need and expenditure (Pedersen, Steensberg et al. 2003) (Pedersen and Febbraio 2008). Such communication partially explains the beneficial effects of physical activity, and one of the most affected tissue is the bone mass (Colaianni, Mongelli et al. 2016). The function of both muscle and bone is intertwined; the bone needs to support the growth of the muscle while the opposite is also true (Brotto and Johnson 2014, Maurel, Jähn et al. 2017). Muscle provides

the mechanical force for the bone to move while the bone provides the core support (Maurel, Jähn et al. 2017).

While for most organs and tissues, the delivery of myokines is through the bloodstream, the bone has also a direct access to these myokines due to the physical proximity of the muscle (Hamrick, McNeil et al. 2010). A study showed that insulin-growth factor 1 (IGF-1) and fibroblast growth factor 1 (FGF-2) - which are two myokines, have their receptors in the bones positioned at the muscle-bone interface, suggesting a myokine movement from the muscle to the bone in a paracrine fashion (Hamrick, McNeil et al. 2010). IGF-1 and FGF-2 were shown to stimulate bone formation by increasing the ability of osteoblast to deposit bone and by promoting osteoblastogenesis, respectively (Hamrick, McNeil et al. 2010). The level of IGF-1 in the serum is in fact an indicator to assess osteoporotic fracture risk in patients (Vandenput, Sjögren et al. 2012).

Another potent myokine that induces bone formation is Irisin. Irisin, which is a potential target of MYF6, although not yet validated (Lazure, Blackburn et al. 2019), is well-studied in the context of the muscle-bone cross-talk (Kim, Wrann et al. 2018) (Colaianni, Sanesi et al. 2019). It was shown that when injecting mice with low dosages of Irisin (once a week, for four weeks), the cortical bone mass and bone mineral density increased in vivo (Colaianni, Cuscito et al. 2015). The mice also displayed a significantly higher bone formation rate (BFR) and mineral apposition rate (MAR) (Colaianni, Cuscito et al. 2015). The same group of researchers cultured osteoblasts in conditioned media (in which primary myoblasts supplemented with serum from active individuals were cultured) and in conditioned media treated with an Irisin antibody (Colaianni, Cuscito et al. 2014). Osteoblasts in the conditioned media with Irisin differentiated, but not when Irisin was absent (Colaianni, Cuscito et al. 2014). They also showed that mRNA levels of alkaline phosphatase (ALP) and collagen type I which are bone pro-formation markers were significantly decreased in the osteoblasts lacking Irisin signalling (Colaianni, Cuscito et al. 2014). Irisin also leads to an increased expression of Osteopontin (OPN), a matrix protein indigenous to the bone that promotes bone formation (Colaianni and Grano 2015).

It has been demonstrated that some interleukins, which are also myokines under the potential control of MYF6 (Lazure, Blackburn et al. 2019) are involved in the maintenance of the bone homeostasis (Levy, Schindler et al. 1996) (Colaianni, Mongelli et al. 2016, Kaji 2016) (Milewska, Domoradzki et al. 2019). Interleukin-6 (IL-6) and Leukemia inhibitory

factor (LIF) stimulate bone resorption by indirectly activating osteoclasts (Yoshitake, Itoh et al. 2008) (Adebanjo, Moonga et al. 1998, Zhang, Wang et al. 2017). IL-6 first induces osteoblasts to produce RANK ligand, which later bind to RANK receptors on the osteoclasts and activate them (Blanchard, Duplomb et al. 2009) (Wu, Zhou et al. 2017). This activation leads to bone remodelling (Wu, Zhou et al. 2017).

1.6- Longitudinal bones characteristics

As previously stated, the skeleton supports the muscle movement by providing a solid core. But the skeleton functions go beyond movement-related ones. Parts of the skeleton protect vital organs from physical damage by forming a rigid barrier between the external environment and the organ (e.g. the skull and the brain; the ribs and the heart and lungs)(Su, Yang et al. 2019) (Clarke 2008). The skeleton is also where haematopoiesis takes place (Taichman 2005, Shen and Nilsson 2012) while serving as a reservoir for calcium and other ions (Boskey and Coleman 2010).

The skeleton of an infant has 270 bones (Huelke 1998), once these bones fuse, their number decreases. Typically, an adult human has 206, not considering extra digits and ribs (Clarke 2008) (Driscoll 2006). Bones fall into different categories depending on their shape (Clarke 2008). These categories are: Longitudinal bones (e.g. tibia and femur), short bones (e.g. carpals and kneecaps), flat bones (e.g. ribs, cranium, ilium, sternum), and irregular bones (e.g. vertebrae, maxilla, coccyx, mandible) (Clarke 2008) (Jepsen 2009). Longitudinal bones, more specifically the femur and the tibia, are the focus of this research.

Typically, long bones have a cortical and trabecular area (Clarke 2008) (Kalenderer Ö. 2016). The cortical area, also called compact bone, is mainly in the diaphysis (hollow shaft) portion of the bone (Kalenderer Ö. 2016). The cortical bone in longitudinal bones is cylindrical and surrounds the medullary space (Kalenderer Ö. 2016). The trabecular area, also called the cancellous bone, is in the extremities, where the metaphysis and epiphysis are. A thin layer of the compact bone surrounds the trabecular area (Kalenderer Ö. 2016). The trabecular area has a honey-comb structure, creating a three dimensional matrix for diverse cells to grow in (Clarke 2008).

Biologically, cortical and trabecular areas are maintained by osteoblasts, osteocytes, and osteoclasts (Clarke 2008, Kalenderer Ö. 2016). All three types of cells are responsible for bone remodelling (Capulli, Paone et al. 2014). While osteocytes and osteoblasts are responsible for bone formation, osteoclasts are responsible for bone resorption (Capulli, Paone et al. 2014). The right balance between the activity of these cell types is crucial for the maintenance of an adequate and healthy bone mass (Capulli, Paone et al. 2014).

Molecularly, bones are made of organic elements (extracellular matrix, lipids, different cell types, growth factors) and inorganic mineral crystals (calcium hydroxyapatite and calcium phosphate) (Boskey and Coleman 2010, Abou Neel, Aljabo et al. 2016). Genetic predispositions and life-style affect bone's morphology, bone mineral density, tissue quality, and mechanistic strength (Jepsen 2009). While sedentarism negatively affect these parameters, physical activity, on the contrary, improves them (Bonaiuti, Shea et al. 2002) (Benedetti, Furlini et al. 2018, Hong and Kim 2018). Exercising stimulates bone remodelling, even in osteoporotic patients (Bonaiuti, Shea et al. 2002) (Benedetti, Furlini et al. 2018). Such beneficial effects are partially explained by myokines (Kaji 2016) (Colaianni, Cuscito et al. 2015, Colaianni, Mongelli et al. 2016).

1.7- Hypothesis and objectives

Skeletal muscle is a contractile tissue which evolved to produce force for movement. However, in metazoans it has also acquired two additional major roles of energy metabolism and endocrine function. The endocrine function of muscle results in production of numerous myokines with local, distal and systemic effects. It was recently discovered that MYF6, also called MRF4, is a master regulator of myokines expression (Lazure, Blackburn et al. 2019). Genetic deletion of *Myf6* leads to significant reduction of many myokines in the serum, raising the possibility that MYF6 may play a role in tissue regeneration and remodelling in other organs such as bone. In this project we use *Myf6* Knockout (KO) animals as a model to study the response of animals to exercise and its effect on bone remodelling and resorption. We have analyzed the role of MYF6 in regulation of osteoblasts and osteoclasts in bone formation and remodelling under normal conditions and during exercise through morphological and mechanical tests.

It is possible that MYF6 is indirectly involved in maintaining the bone mass and overall health of the bones post development through the action of its secreted myokines. We hypothesized that the loss of MYF6 adversely affect bone remodelling and resorption due to the decrease in expression of key myokines - some of which are involved in bone regeneration. And since MYF6 expression is upregulated following exercise, we also hypothesized that consistent physical activity might enhance the benefits of these myokines in WT mice compared to their *Myf6*-KO counterparts.

Aims:

Aim 1 : Bone Characterization at a Steady-State

1.1 – Analysis of bone's structural properties of the tibia

Micro Computed Tomography (microCT)

1.2 –Analysis of mechanical properties of the femur

Three-point bending test (TPB)

Aim 2 : Bone Characterization following physical training

2.1 – Analysis of bone's structural properties of the tibia

Micro Computed Tomography (microCT)

2.2 –Analysis of mechanical properties of the femur

Three-point bending test (TPB)

Chapter 2: Materials and Methods

2.1- Cohort description

Two main cohorts are used for this study: A steady state cohort and an active cohort made of control and *Myf6*- KO mice. The steady-state cohort is defined as mice at rest, without any change in their diet or level of physical activity. WT or heterozygous (Het) for *Myf6* mice were used as controls (refer to the appropriate section for more details). *Myf6*-KO mice have a cassette inserted into the first exon of the gene, rendering it null (Fig S1).

All mice used in this study are male, of more than 3 months in age (refer to appropriate section for exact age) - time at which the reduction in myokines is significantly detected between the control and *Myf6*-KO mice. The specific age is mentioned for every experiment. The mice were housed under a 12-h light/dark cycle. The active mice are mice that followed an endurance swimming test, spanning 9 weeks. The mice were exercised and euthanized according to the protocols that were approved by the Animal Care Committee of both McGill University and the Lady Davis Institute.

2.2- Endurance swimming program

The swimming program is derived from the training that was described before, with some modifications (Barhoumi, Briet et al. 2014). Briefly, 4 male heterozygous mice (control) and 4 male *Myf6*-KO mice (3 months-old) were put in a tank and forced to swim for 60 minutes every morning, 5 days a week. The program lasted 9 weeks in total, including one week of conditioning. Conditioning allowed for the mice to adapt to this new environment. Over 5 days, the swimming time was increased regularly, starting from 10 minutes to 60 minutes a day. The swimming time for the following 8 weeks was kept at 60 minutes a day.

As mice consider the tank a new territory to be dominated, only four mice were exercised together to avoid violent behaviour. The mice were supervised at all time. Although it is normal for mice to go under water, mice were taken out of the tank if they stayed under water for more than four seconds (which is life-threatening). They were not returned to the

swimming tank for the rest of the day and allowed to rest. Such an event happened only once throughout the 9 weeks of exercising.

To avoid the mice from staying immobile in the water, a continuous stream of bubbles produced by an aerator line was added to the system. The water levels were high enough for the mice not to be able to stand on their tails. The water was kept at 37°C throughout the time the mice were in the tank.

Out of the four mice swimming in the tank, two were controls and two were *Myf6*-KO to avoid miscellaneous (not accounted for) events during the swimming sessions to affect one cohort and not the other. Following every session, the mice were first dried by hand, with a towel, then put in an incubator which was pre-set at 34°C for 20 minutes. Food and water were provided in the incubator. The mice were then returned to their racks.

2.3- Bone preparation for microComputed tomography (mircoCT) analysis

Steady-state. The tibias were extracted from 16 mice (4 months old) – 8 are WT and 8 are *Myf6*-KO. They were sacrificed directly before the dissection. The bones were cleaned thoroughly, removing as much muscle and tendons attached to them. The fibulae were kept attached to the cortical bone. The bones were then put in saline (PBS) water and wrapped in drenched gauze. The bones were stored in -80°C freezer until needed.

Active state. The tibias were extracted from 8 mice (5 months old) – 4 are heterozygous and 4 are *Myf6*-KO. They were sacrificed directly before the dissection. The bones were cleaned thoroughly, removing as much muscle and tendons attached to them. The fibulae were kept attached to the cortical bone. The bones were then put in saline (PBS) water and wrapped in drenched gauze. The bones were stored in -80°C freezer until needed.

2.4- MicroCT ex-vivo scans, 3D reconstruction, and analysis of the tibias

Steady-state and active state. The bones were scanned using the Skyscan 1272, version 1.1.19 (manufactured by Brucker, U.S.A). The parameters of the scans were: scaled image pixel size (um)=5.000091, resolution = 2452 x 1640, rotation step (deg)=0.400, filter=Al 0.5mm, exposure (ms)=1750, scanning position=54.000 mm. The parameters of the

X-ray were: source voltage (kV)= 61, source current (uA)= 162. The pictures were taken mid-shaft (right below the third trochanter) and no adjustment for the bone size was needed.

To reconstruct and view the bones, three software were used. The reconstruction Program NRecon, version 1.6.10.4, was used to select the vertical (proximal to distal) volume of interest based on the scans. Data Viewer was used to rotate the sample and finally, CTAn was used to analyse the images after separately segmenting the cortical (100 slides in total, 75 slides above where the fibula and tibia merge) and trabecular (200 slides in total, 50 slides below the primary spongiosa) regions of interests with custom processing techniques.

2.5- Bone preparation for three-point bending test

Steady-state. The femurs were extracted from 16 mice (4 months old) – 8 are WT and 8 are *Myf6*-KO. They were sacrificed directly before the dissection. The bones were cleaned thoroughly, removing as much muscle and tendons as possible, and any associated knee or hip joint. The bones were then put in saline (PBS) water and wrapped in drenched gauze. The bones were stored in -80°C freezer until needed.

Active state. The femurs were extracted from 8 mice (5 months old) – 4 are heterozygous and 4 are *Myf6*-KO. They were sacrificed directly before the dissection. The bones were prepared as described for the steady-state.

2.6- Three-point bending test

Steady-state and active state. The bones were subjected to a mechanical load using the Instron 5943 machine, manufactured by Instron. There was a 7mm distance between the two vertical supports – in accordance with the age of the mice and recommended manufacturer protocol. The femurs were placed in the anteroanterior (AP) direction. The load was applied to the mid-point area of each bone (peak stress is located at the material mid-point with reduced stress elsewhere). The load is applied perpendicularly to the longitudinal axis of the bone. The bones were loaded until failure (breaking point). The stiffness was defined as the linear regression of the loading graph.

2.7- Statistical analysis of the microCT data

The statistical analysis was performed through GraphPad Prism 8.2.1 (441). The unpaired two-tailed t-test was declared statistically significant between the control and the *Myf6*-KO group if the p-value was below 0.05 ($p < 0.05$). Error bars are for the standard deviation within the same group. Asterisks (*, **, ***, ****) correspond to p-values of <0.05, <0.01, <0.001 and <0.0001, respectively.

2.8- Statistical analysis of the three-point bending data

The statistical analysis was performed through GraphPad Prism 8.2.1 (441). The unpaired two-tailed t-test was declared statistically significant between the control and the *Myf6*-KO group if the p-value was below 0.05 ($p < 0.05$). Error bars are for the standard deviation within the same group. Asterisks (*, **, ***, ****) correspond to p-values of <0.05, <0.01, <0.001 and <0.0001, respectively. The values were adjusted to weight using the linear regression method. To adjust the values to their corresponding weight, the formula below has been used:

Trait (adjusted)i = Trait (unadjusted)i –[(Slope (trait vs body mass)*(body mass i – Mean body mass)]

Chapter 3: Results

3.1- MicroCT data

The analysis of the bones' structural properties was undertaken through micro computed tomography (microCT) of both the cortical and the trabecular areas of the tibias. The imaging was performed at a resolution of 5 microa (pixel size), mid-shaft, right below the third trochanter. MicroCT is a 3D imaging technique. The scanner takes multiple x-ray images on a two-dimensional plane, which are later reconstructed into 3D images.

3.1.1 - Steady-state:

The cohorts consisted of 8 WT and 8 *Myf6*-KO male mice. The mice were at steady-state (at rest) and were 4 months old at the time of the bone collection. The results of the two-dimensional (2D) cortical analysis of the tibias are shown in **Figure 1**. The results of the cortical porosity analysis of the tibias are shown in **Figure 2**. The results of the trabecular analysis of the tibias are shown in **Figure 3.** Each dot is a data point for one mouse.

The 2D cortical analysis shown in **Figure 1** is the analysis of the cross-sectional properties of the cortical bone of 8 biological replicates (aged 4months old), at middiaphysis. These parameters include the total cross-sectional area inside the periosteal envelope (Tt.Ar) (F1.a), the cortical bone area (Ct.Ar) (Fig1.b), the medullary area (Ma.Ar) (Fig1.c), the cortical area fraction (CtAr/Tt.Ar) (Fig 1.d), the cortical thickness (Ct.Th) (Fig 1e), the periosteal perimeter (Ps.Pm) (Fig 1. f), the endocortical perimeter (Ec,Pm) (Fig 1. g), the maximum moment of inertia (Imax) (Fig 1. h), and the minimum moment of inertia (Imin) (Fig 1. i).

The total bone area (Tt.Ar) is the area including the cortical bone (Ct.Ar) and the marrow areas (Ma.Ar), inside the periosteal envelope (Jepsen, Silva et al. 2015) (Bouxsein, Boyd et al. 2010). While the cortical bone is made of solid bone, the marrow area is made of red and yellow marrow (Cooper 2011). The cortical thickness (Ct.Th) and the cortical area (Ct.Ar) are used to assess the net amount of bone present in the diaphysis of the bone (Jepsen, Silva et al. 2015).

The morphological data is important in showing if either the marrow or the bones were affected by the loss of MYF6. These parameters are the reflexion of the cellular activity taking place in these defined areas (Jepsen, Silva et al. 2015) (Bouxsein, Boyd et al. 2010).

Minimal moment of inertia (Imin) is the moment of inertia of the bone relative to the axis for which it is the least stiff, and maximum amount of inertia (Imax), is the moment of inertia of the bone relatively to the axis for which the bone is the most stiff. These two parameters are used to anticipate the mechanistic performance of the bones (Jepsen, Silva et al. 2015). The endosteal (or endocortical) and periosteal perimeters are the outside layer of the medullary area and compact bone, respectively.

Figure 1 shows that none of these parameters (Fig1 a-i) are significant between the two cohorts, meaning that the loss of MYF6 did not affect the bones' geometric properties in mice that are at rest (steady-state).

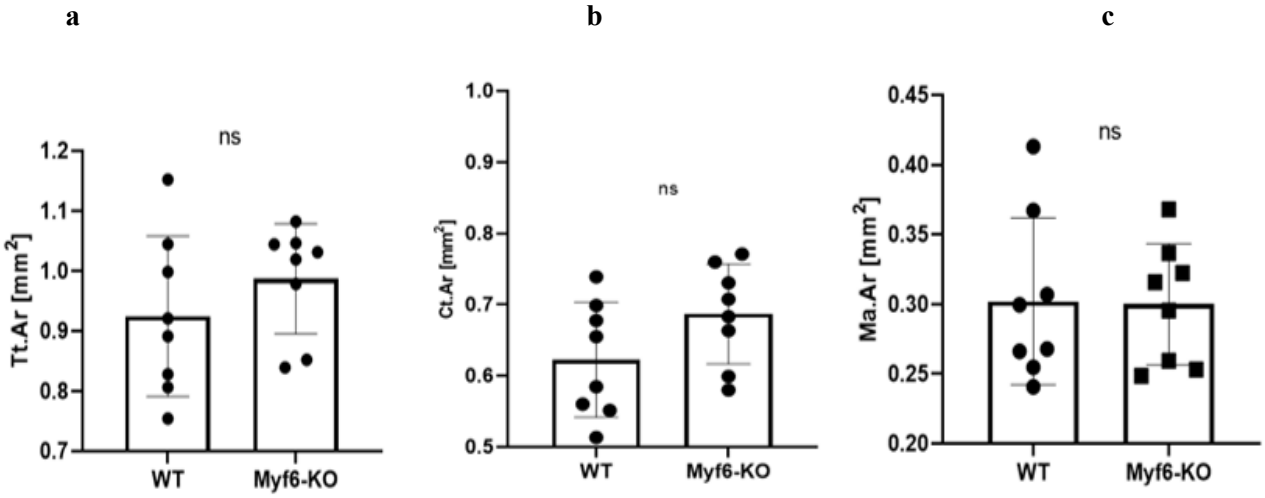

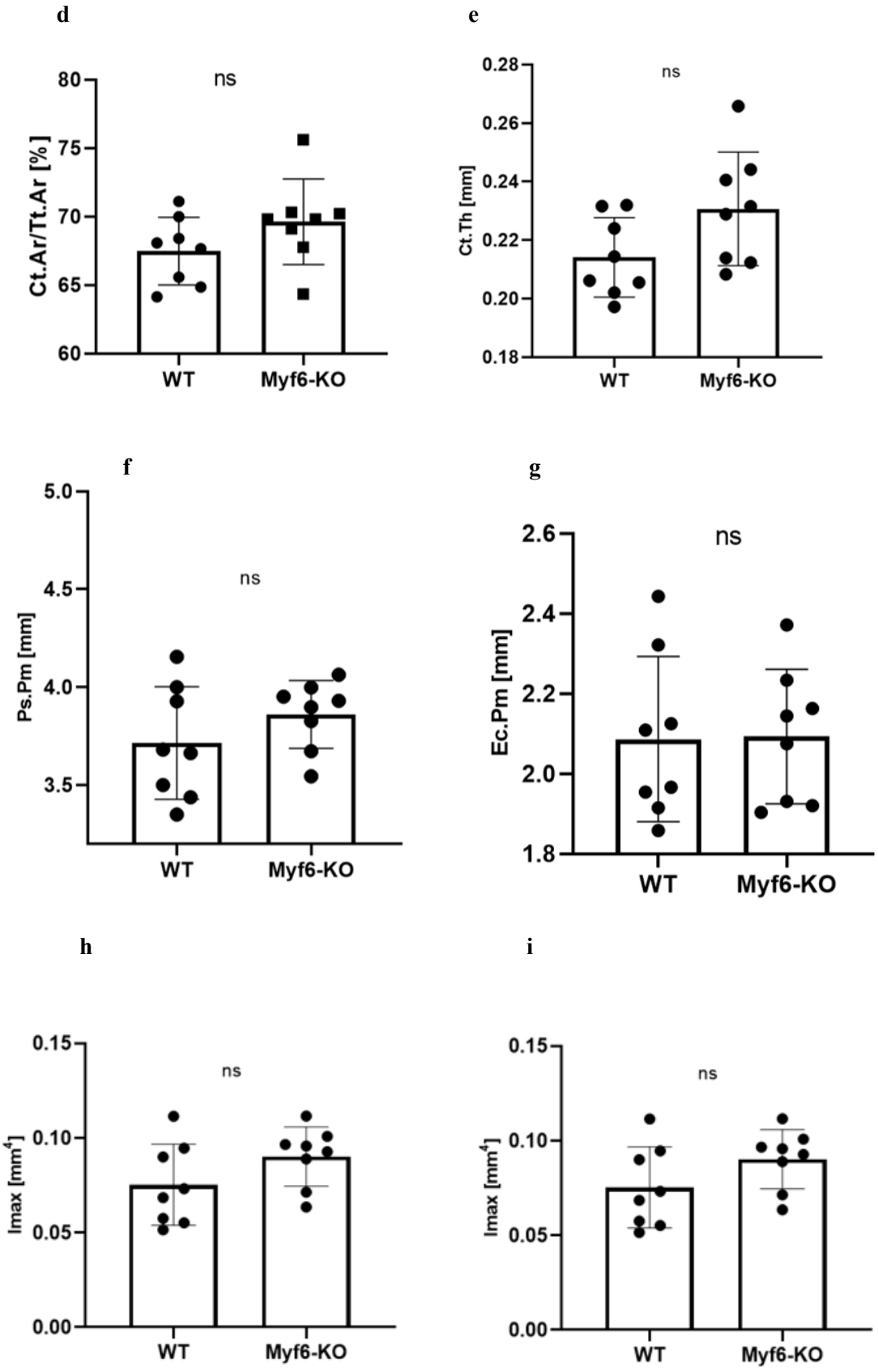
d
ns
80
75
70
65
60
Ct.Ar/Tt.Ar [%]
WT
Myf6-KO
e
ns
0.28
0.26
0.24
0.22
0.20
0.18
Ct.Th [mm]
WT
Myf6-KO
f
ns
5.0
4.5
4.0
3.5
Ps.Pm [mm]
WT
Myf6-KO
g
ns
2.6
2.4
2.2
2.0
1.8
Ec.Pm [mm]
WT
Myf6-KO
h
ns
0.15
0.10
0.05
0.00
Imax [mm4]
WT
Myf6-KO
i
ns
0.15
0.10
0.05
0.00
Imax [mm4]
WT
Myf6-KO

j **k**

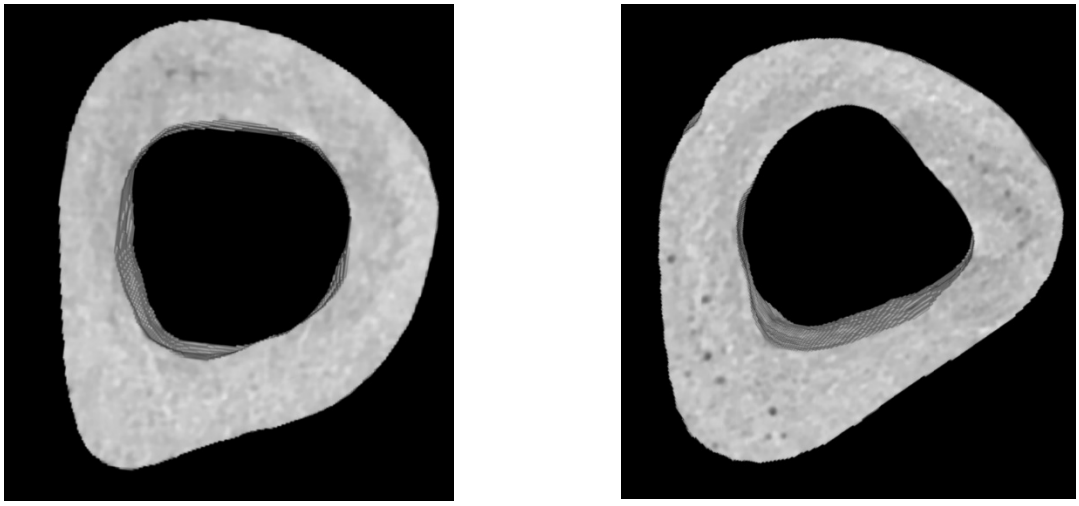

Figure 1: Two-dimensional cortical analysis of the tibia at steady state. **a-** Total cross-sectional area inside the periosteal envelope (Tt.Ar), **b-** Cortical bone area (Ct.Ar), **c -** Medullary area (Ma.Ar), **d-** Cortical area fraction (CtAr/Tt.Ar), **e-** Cortical thickness (Ct.Th), **f-** Periosteal perimeter (Ps.Pm), **g-** Endocortical perimeter (Ec,Pm), **h-** Maximum moment of inertia (Imax), **i-** Minimum moment of inertia (Imin). **j-** Representative image of a WT cortical bone. **k-** Representative picture of a *Myf6*-KO cortical bone. N=8 biological replicates.

Figure 2 is the analysis of the cortical porosity of the steady-state mice, aged 4 months old. Total pore volume (Po.V) is the total volume occupied by pores in the volume of interest (VOI) (Fig2.a). The cortical porosity in the selected area (Ct.Po) is the percentage that those pores represent of the entire bone volume as described in Fig2.b. The number of closed pores in the selected area (Po.N) are the pores that are not blood vessels (Fig2.c).

The results in **Figure 2** show that both the total pore volume (Po.V) and the cortical porosity (Ct.Po) are significantly different between the two cohorts. The *Myf6*-KO mice have a higher porosity compared to the wild-type (Fig2a-b). However, the number of closed pores is not significant between the two cohorts.

a

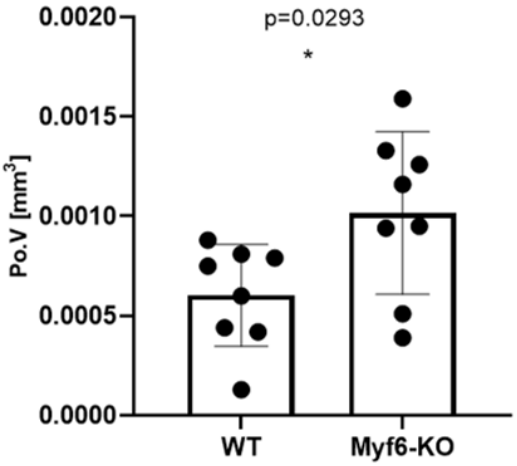
p=0.0293
*
0.0020
0.0015
0.0010
0.0005
0.0000
Po.V [mm3]
WT
Myf6-KO

b

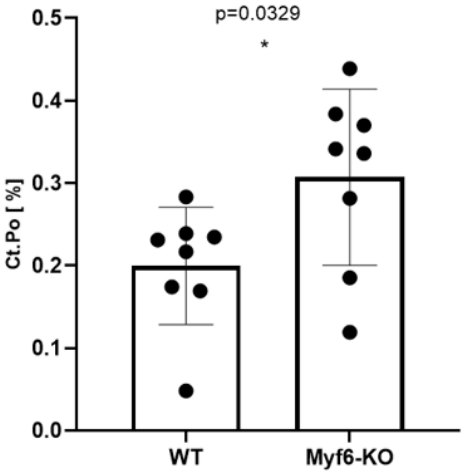
p=0.0329
*
0.5
0.4
0.3
0.2
0.1
0.0
Ct.Po [%]
WT
Myf6-KO

c

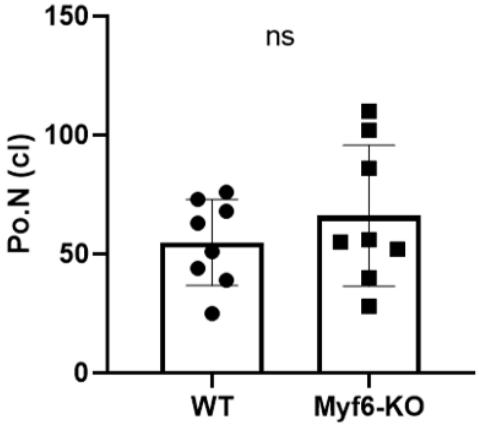
ns
150
100
50
0
Po.N (cl)
WT
Myf6-KO

d **e**

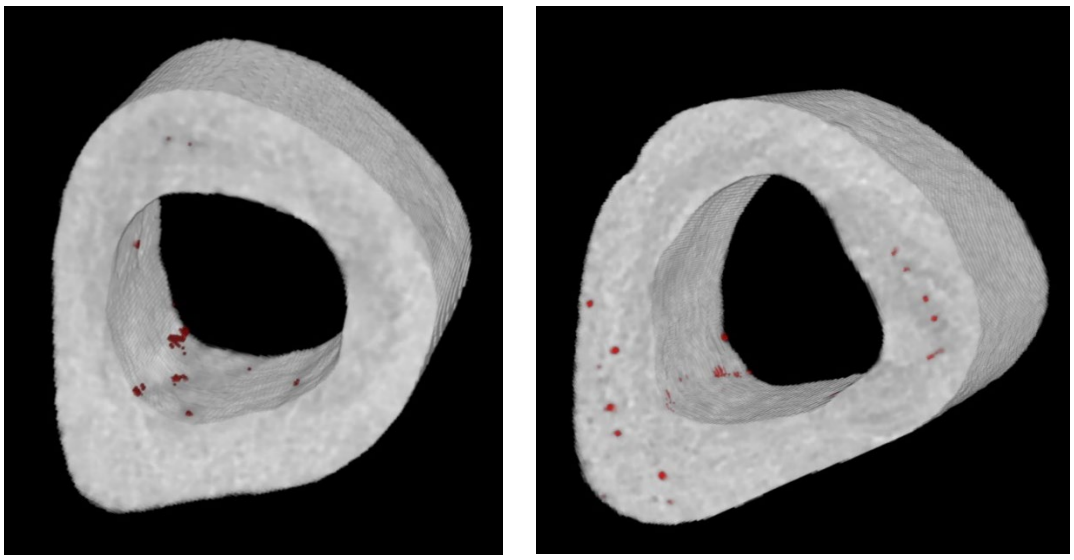

Figure 2: Cortical porosity analysis of the tibia at steady state. a- Total pore volume (Po.V), **b –** Cortical porosity in the selected area (Ct.Po), **c-** Number of closed pores in the selected area (Po.N). **d-** Representative image of a WT cortical bone porosity. **e-** Representative picture of a *Myf6*-KO cortical bone porosity. N=8 biological replicates.

Figure 3 is the trabecular bone architecture data at steady-state. The total volume of the region of interest (TV) (Fig3.a) is the volumetric measure of the region that was selected for the micro-CT analysis. The bone volume of the selected region (BV) (Fig3.b) is the total volume minus the volume of the medullary area – which is bone marrow. The bone surface of the selected region (BS) (Fig3.c) is the area occupied by the bone on a two-dimensional plane. The ratio of the bone volume to the total volume in the region of interest (BV/TV) (Fig3.d) is used to determine the contribution of the bone mass to the entire volume (bone volume fraction). The ratio of the bone surface to the bone volume in the region of interest (BS/BV) (Fig3.e) is an index for specific bone surface. The trabecular number (Th.N), trabecular thickness (Th.Th), and trabecular separation (Th.S) (Fig3. f-h) are parameters

describing the trabeculae meshwork. The structure model index (SMI) (Fig3.i) is an indicator of the overall shape (plate or rod) of the trabecular area (SMI = 4 refers to a more spherical shape, SMI=3 to cylindrical ones, and SMI= 0 to planar shape) (Salmon, Ohlsson et al. 2015) . The degree of anisotropy (DA) (Fig3.j) is a measure to determine how highly oriented the subarchitecture of the trabecular bone is (0 = isotropic, 1 = anisotropic) (Kersh, Zysset et al. 2013).

From **Figure 3** we can note that none of the parameters are significant between the two cohorts at steady state. This means that the overall architecture of the trabecular bone in the tibia of these mice is similar in terms of volume, ratios, shape, and orientation - and is not affected by MYF6 loss.

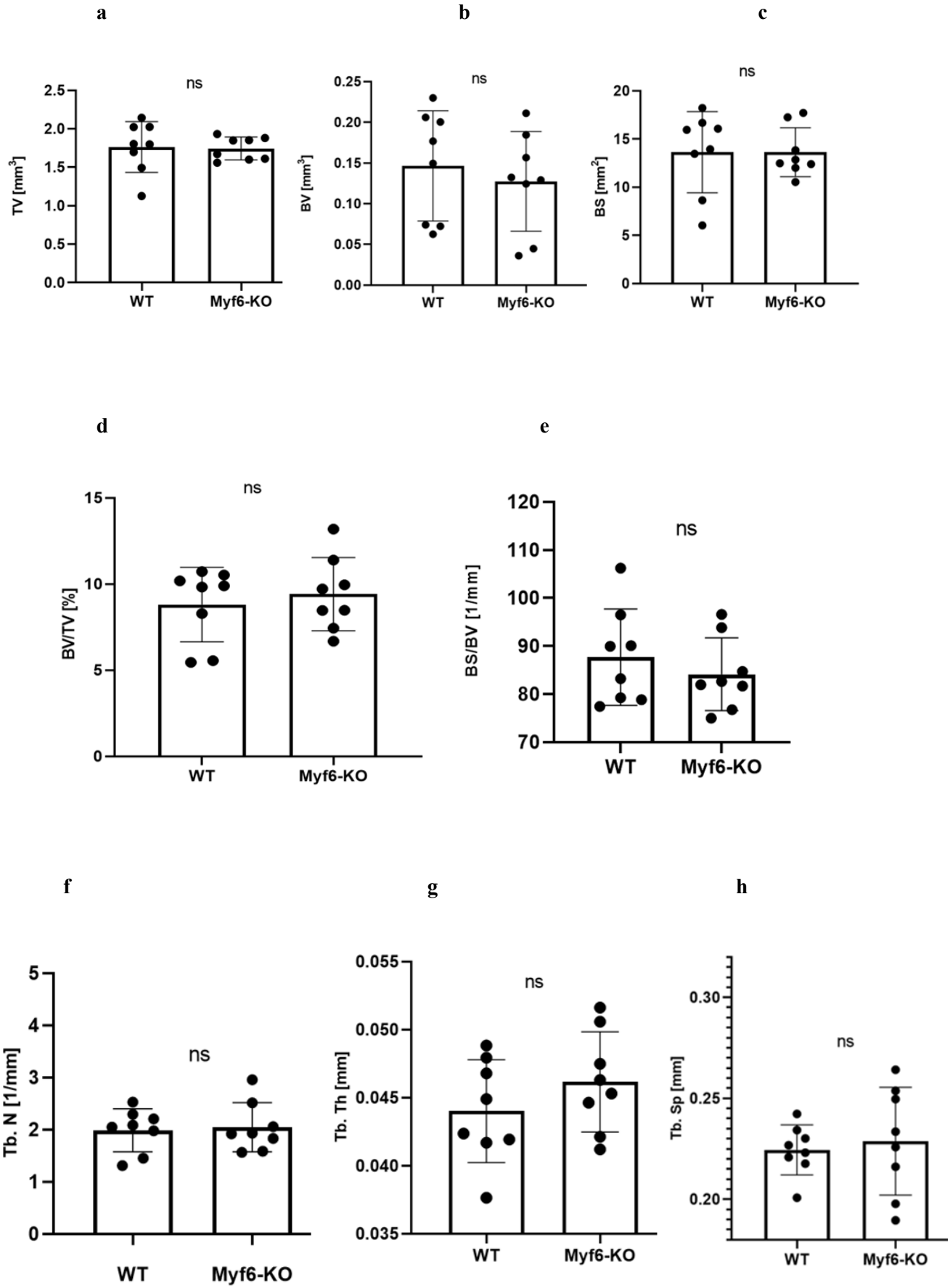
a
b
c
ns
TV [mm³]
BV [mm³]
BS [mm²]
WT
Myf6-KO
d
e
BV/TV [%]
BS/BV [1/mm]
f
g
h
Tb. N [1/mm]
Tb. Th [mm]
Tb. Sp [mm]

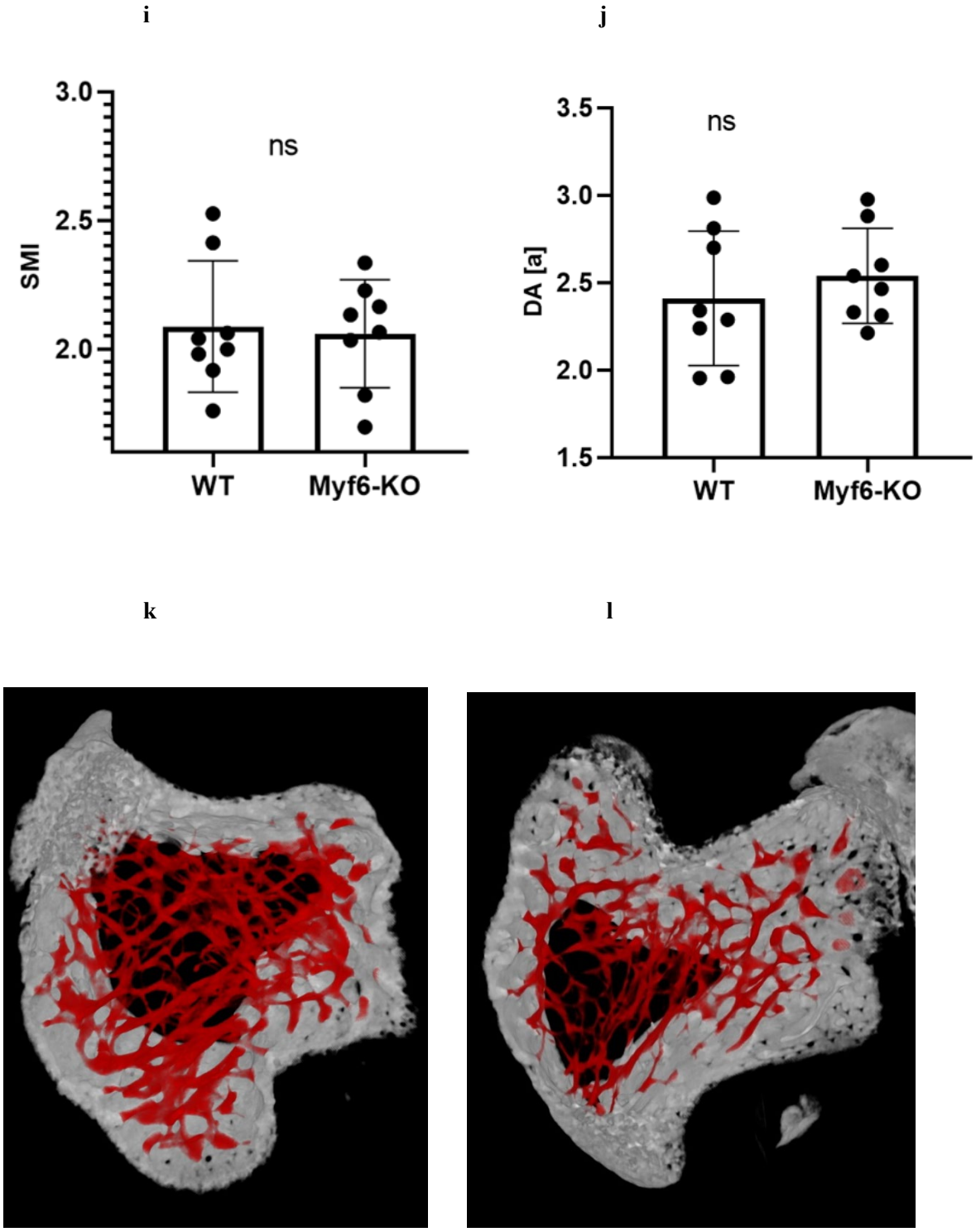

Figure 3: Trabecular analysis of the tibia at steady-state. **a-** Total volume of the region of interest (TV), **b-** Bone volume of the selected region (BV), **c-** Bone surface of the selected region (BS), **d-** Ratio of the bone volume to the total volume in the region of interest (BV/TV), **e-** Ratio of the bone surface to the bone volume in the region of interest (BS/BV), **f**

– Trabecular number (Th.N), **g-** Trabecular thickness (Th.Th), **h-** Trabecular separation (Th.S), **i –** Structure model index (SMI), **j-** Degree of anisotropy (DA). **k-** Representative image of a WT trabecular section. **l-** Representative picture of a *Myf6*-KO trabecular section. N=8 biological replicates.

3.1.2 - Active state:

Four heterozygous and four *Myf6*-KO, age and sex matched (male) mice were exercised for 9 weeks. The physical training consisted of an exhaustive swimming test spanning 8 weeks, plus one additional week of conditioning at the beginning, 5 days a week, 1h daily. Swimming was an ideal exercise since the physical activity is maintained in hypogravity (Gomez-Bruton, Gonzalez-Aguero et al. 2016), with only a minimal impact on the bone themselves.

The results of the two-dimensional cortical analysis of the tibias following the swimming training are shown in **Figure 4**. The results of the cortical porosity analysis of the tibias are shown in **Figure 5**. The results of the trabecular analysis of the tibias are shown in **Figure 6.** Each dot is a data point for one mouse.

In **Figure 4**, the parameters which were previously described (same as Fig2) are not significant between the two cohorts (the mice are 5 months old). This means the loss of MYF6 did not change the cortical features of the bones, even when the mice are active and MYF6 is upregulated. One is to also note that the variation in the heterozygous cohort (control) is wider compared to the *Myf6*-KO, which is more compacted.

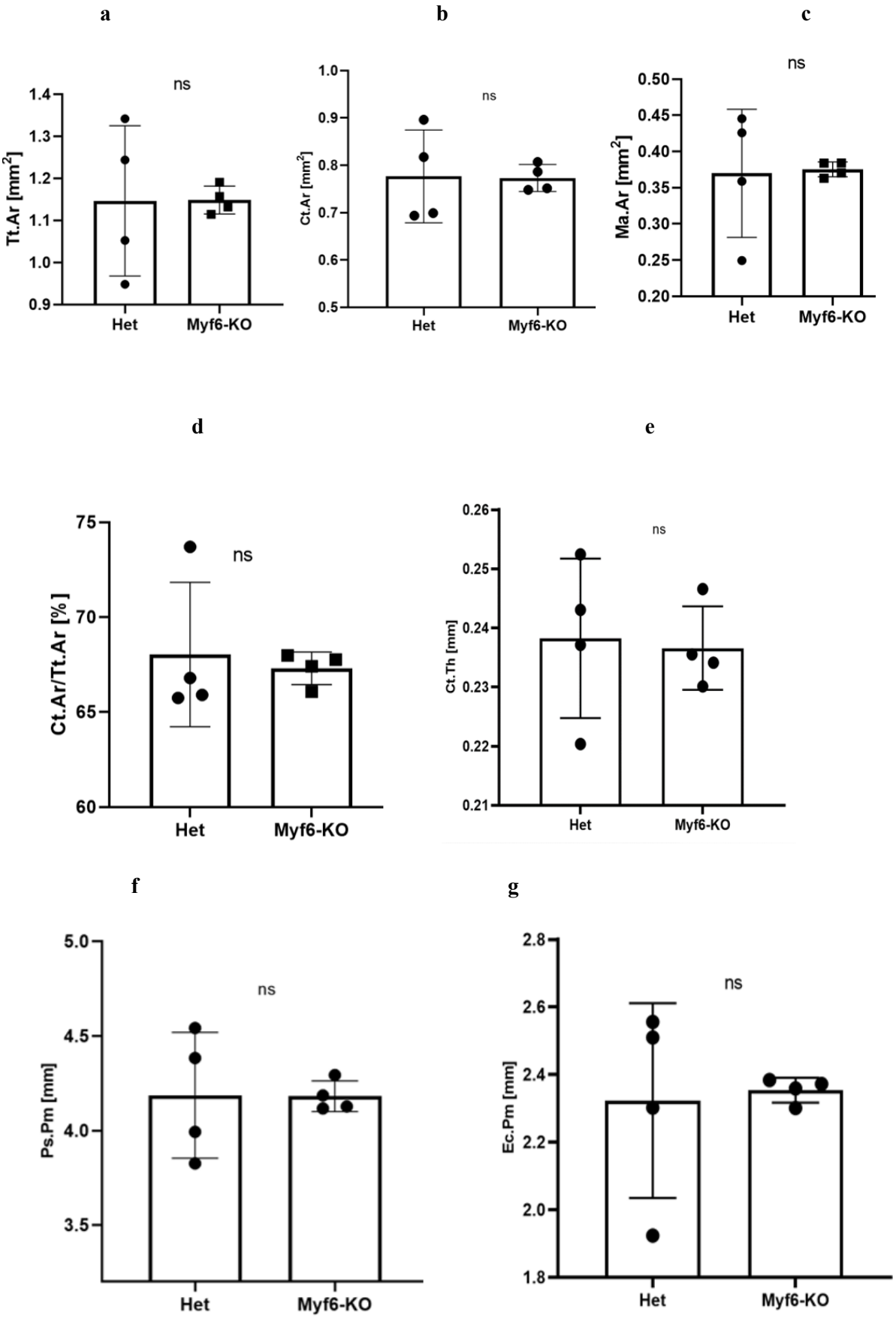
a
b
c
ns
ns
ns
Tt.Ar [mm2]
Ct.Ar [mm2]
Ma.Ar [mm2]
1.4
1.3
1.2
1.1
1.0
0.9
1.0
0.9
0.8
0.7
0.6
0.5
0.50
0.45
0.40
0.35
0.30
0.25
0.20
Het
Myf6-KO
Het
Myf6-KO
Het
Myf6-KO
d
e
ns
ns
Ct.Ar/Tt.Ar [%]
Ct.Th [mm]
75
70
65
60
0.26
0.25
0.24
0.23
0.22
0.21
Het
Myf6-KO
Het
Myf6-KO
f
g
ns
ns
Ps.Pm [mm]
Ec.Pm [mm]
5.0
4.5
4.0
3.5
2.8
2.6
2.4
2.2
2.0
1.8
Het
Myf6-KO
Het
Myf6-KO

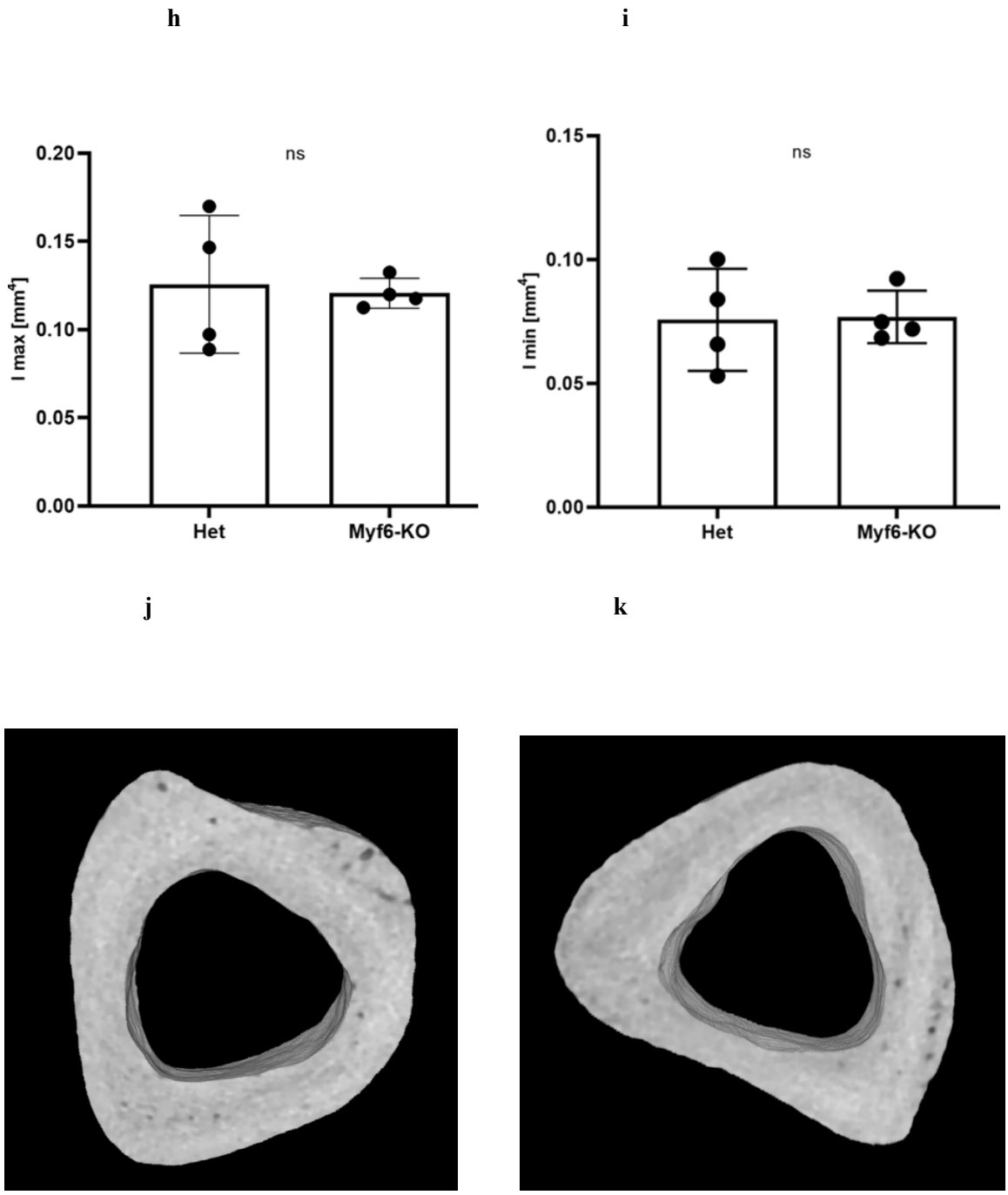

Figure 4: Two-dimensional cortical analysis of the tibia at active state. a- Total cross-sectional area inside the periosteal envelope (Tt.Ar), **b-** Cortical bone area (Ct.Ar), **c -** Medullary area (Ma.Ar), **d-** Cortical area fraction (CtAr/Tt.Ar), **e-** Cortical thickness (Ct.Th), **f-** Periosteal perimeter (Ps.Pm), **g-** Endocortical perimeter (Ec,Pm), **h-** Maximum moment of inertia (Imax), **i-** Minimum moment of inertia (Imin). **j-** Representative image of a *Myf6*-heterozygous cortical bone. **k-** Representative picture of a *Myf6*-KO cortical bone. N=4 biological replicates.

Figure 5, which represents the cortical porosity data for the active cohorts, shows no difference between the two cohorts in terms of porosity, as opposed to the steady-state.

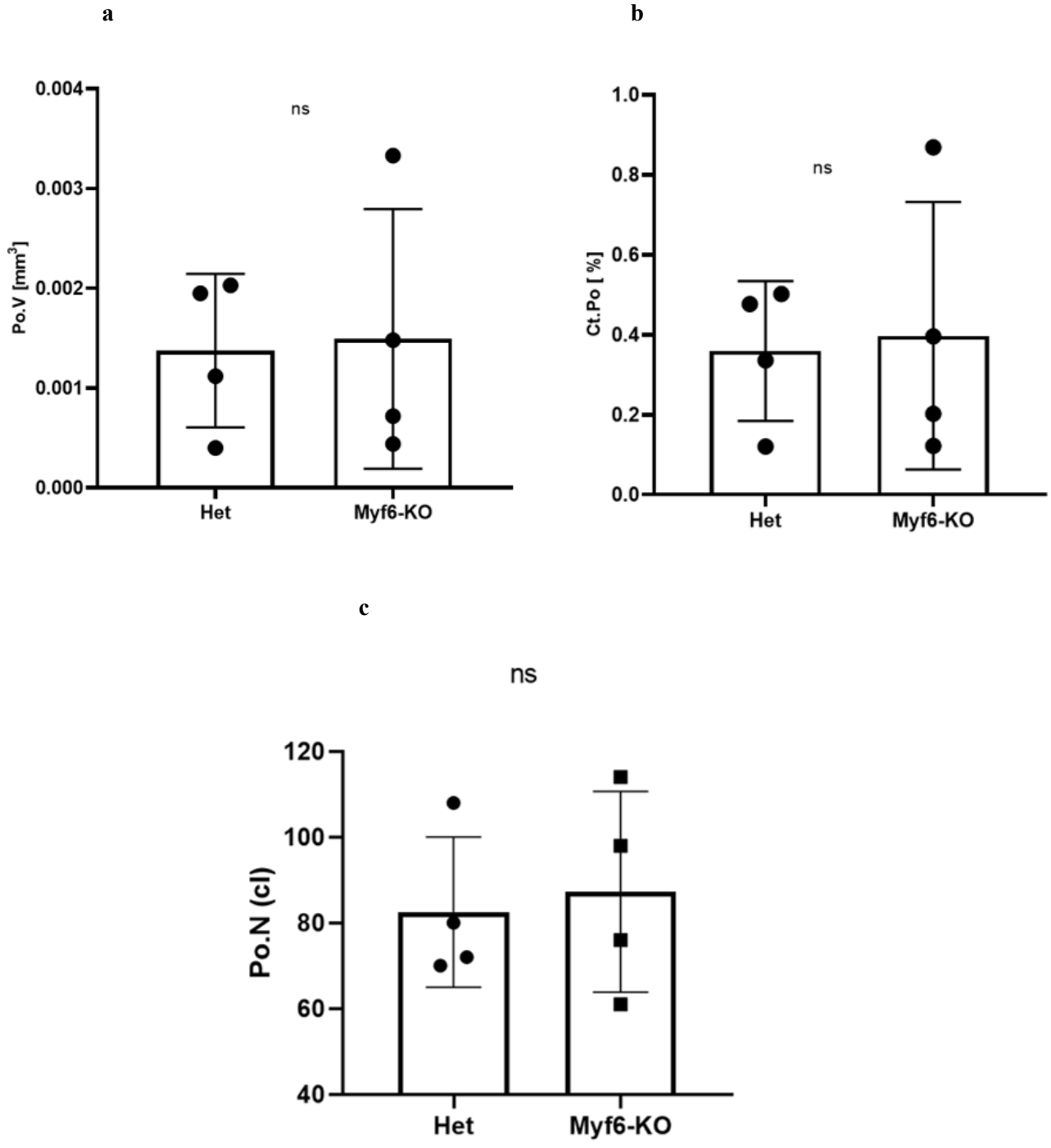

d **e**

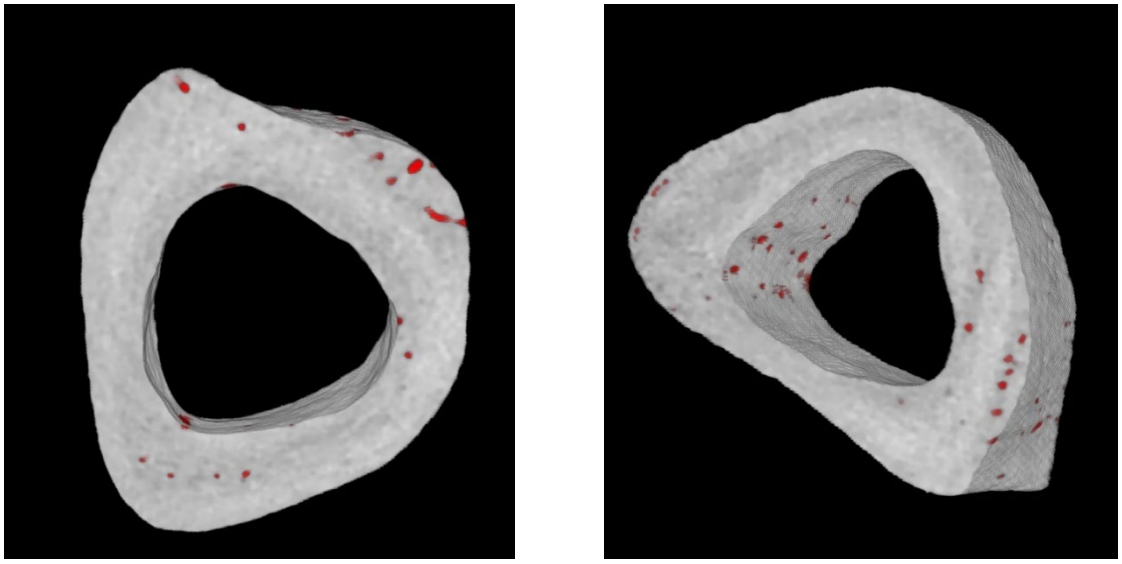

Figure 5: Cortical porosity analysis of the tibia at active state .a- Total pore volume (Po.V), **b –** Cortical porosity in the selected area (Ct.Po), **c-** Number of closed pores in the selected area (Po.N). **d-** Representative image of a WT cortical bone porosity. **e-** Representative picture of a *Myf6*-KO cortical bone porosity. N=4 biological replicates.

Figure 6 is the trabecular bone architecture analysis of the active cohort. The trabecular parameters that were also explained earlier are not significant between the two cohorts (mice are 5 months old), suggesting that the lack of upregulation of MYF6 in the *Myf6*-KO mice following exercise does not affect the morphological features of the tibias.

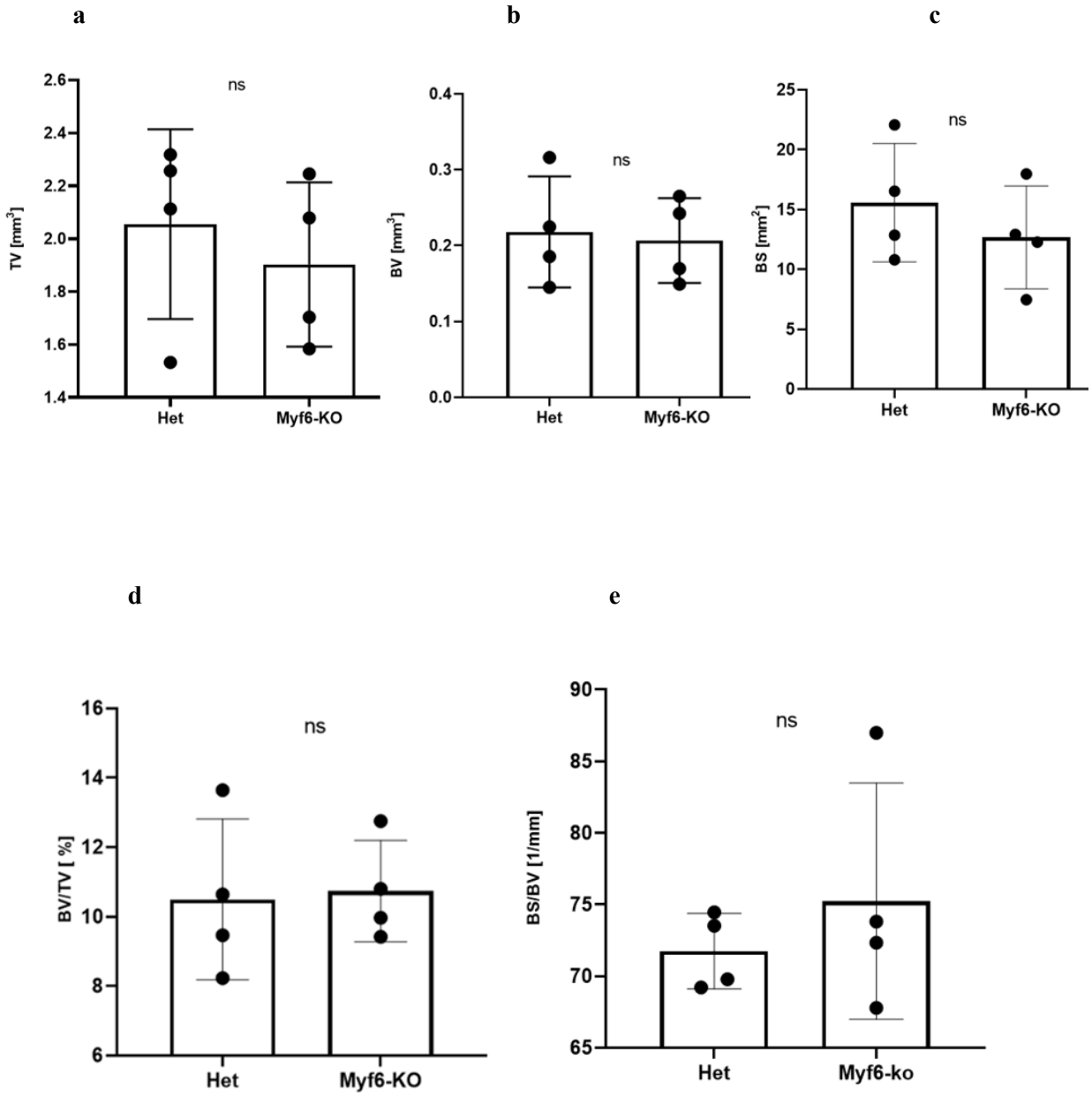
a
b
c
ns
ns
ns
TV [mm³]
BV [mm³]
BS [mm²]
2.6
2.4
2.2
2.0
1.8
1.6
1.4
0.4
0.3
0.2
0.1
0.0
25
20
15
10
5
0
Het
Myf6-KO
Het
Myf6-KO
Het
Myf6-KO
d
e
ns
ns
BV/TV [%]
BS/BV [1/mm]
16
14
12
10
8
6
90
85
80
75
70
65
Het
Myf6-KO
Het
Myf6-ko

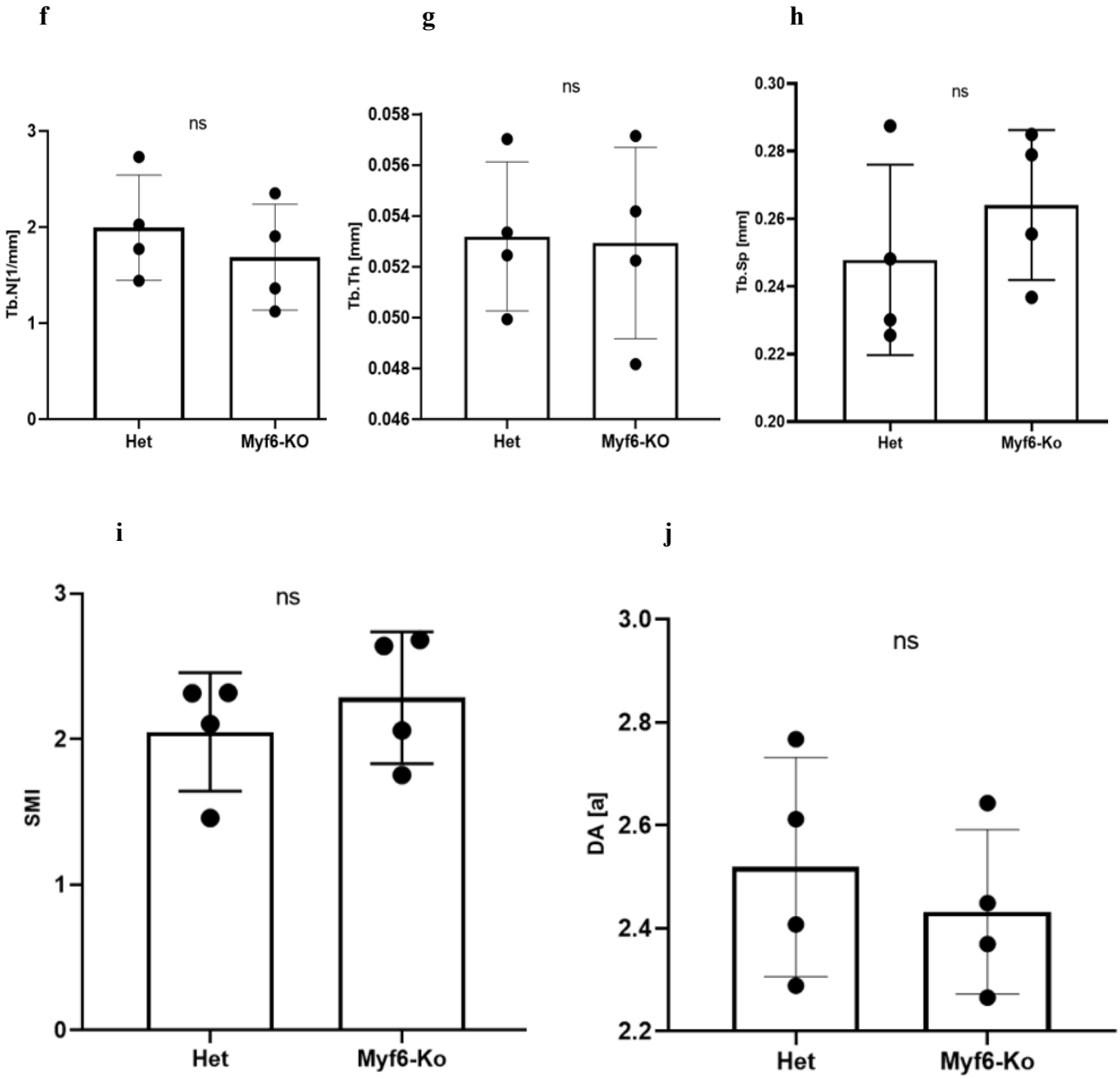
f
g
h
ns
Tb.N[1/mm]
Tb.Th [mm]
Tb.Sp [mm]
Het
Myf6-KO
Myf6-Ko
i
j
SMI
DA [a]

k **l**

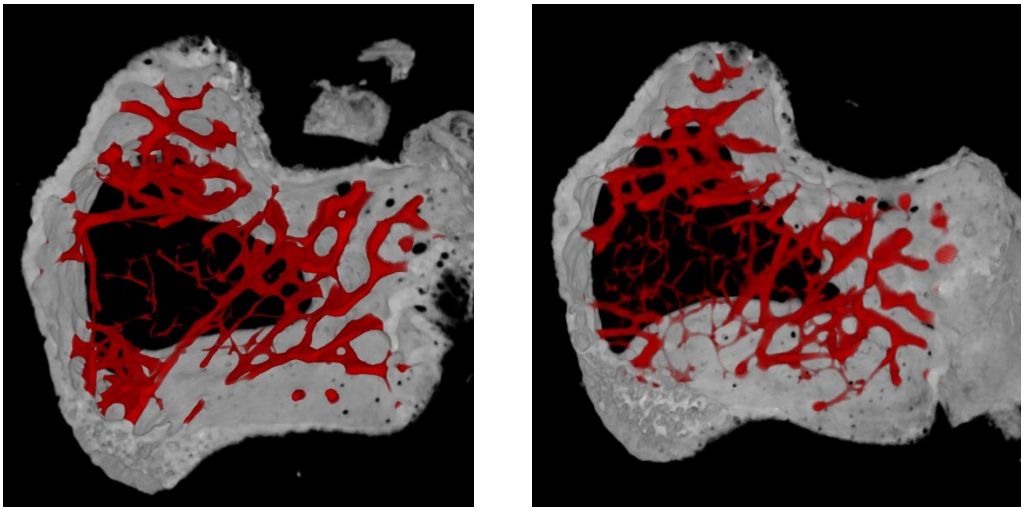

Figure 6: Trabecular analysis of the tibia at active-state. a- Total volume of the region of interest (TV), **b-** Bone volume of the selected region (BV), **c-** Bone surface of the selected region (BS), **d-** Ratio of the bone volume to the total volume in the region of interest (BV/TV), **e-** Ratio of the bone surface to the bone volume in the region of interest (BS/BV), **f –** Trabecular number (Th.N), **g-** Trabecular thickness (Th.Th), **h-** Trabecular separation (Th.S), **i –** Structure model index (SMI), **j-** Degree of anisotropy (DA). N=4 biological replicates. **k-** Representative image of a heterozygous-*Myf6* trabecular section. **l-** Representative picture of a *Myf6*-KO trabecular section N=4 biological replicates.

3.2- Three-point bending test data

Analysis of the mechanistic properties of the bones (femur) was performed through a three-point bending test. The test consists of applying a load perpendicularly to the longitudinal axis, at mid-point of the bone -femur in this case - while maintaining reduced stress on the extremities.

Three-point bending analysis measures different parameters on two levels: whole bone and tissue level. Most values need to be adjusted to body size because bigger mice tend to have bigger bones (Jepsen, Silva et al. 2015). To avoid misinterpreting the size of bones and their mechanical properties, accounting for body size is a necessary step in reporting the major parameters (Jepsen, Silva et al. 2015).

Stiffness is the slope of the linear portion of the load-displacement curve (Jepsen, Silva et al. 2015). The stiffer a bone, the steeper the slope (Jepsen, Silva et al. 2015). The maximum load is the greatest load recorded before a macrofracture is detected (Jepsen, Silva et al. 2015). Work to break is the area underneath the load-displacement curve, from the beginning of the test up the breaking point (Funk, Kerrigan et al. 2004). The post-yield displacement is the difference between the displacement (difference in bone length) at yield and the displacement at break (Jepsen, Silva et al. 2015). The higher the post-displacement yield, the stronger the bone.

The results of the three-point bending test are shown in **Figure 7** for the steady-state cohort while the active cohort results are shown in **Figure 8.**

3.2.1- Steady-state:

The results in Figure 7 show that there is no significant difference between the two cohorts at steady-state in terms of mechanistic performance. The loss of MYF6 does not seem to affect the mechanistic properties of the femur. One is also notice that the trend of the values in on the higher side for the *Myf6*-KO mice, suggesting that the *Myf6*-KO mice might be on the stronger side, although on statistical terms, there is no difference between the two cohorts.

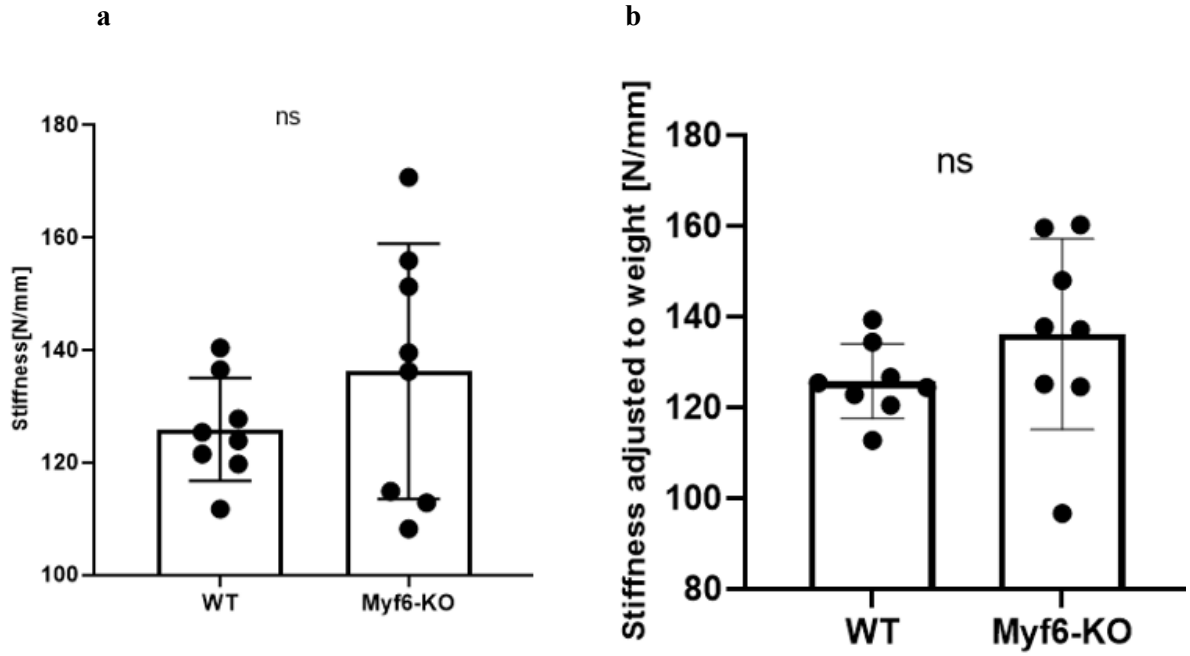

c

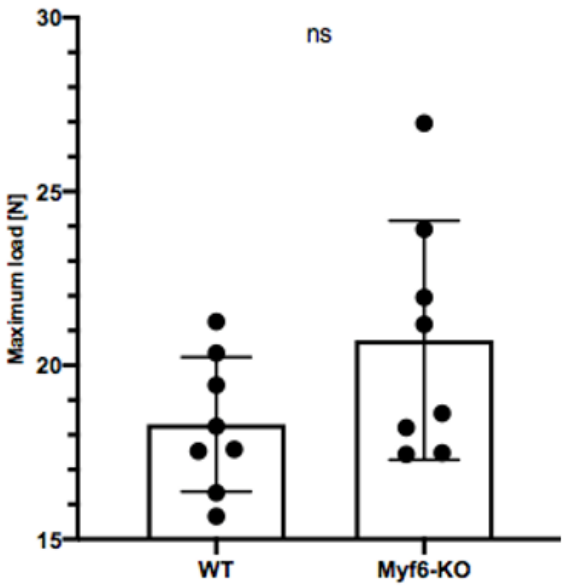
ns
Maximum load [N]
30
25
20
15
WT
Myf6-KO

d

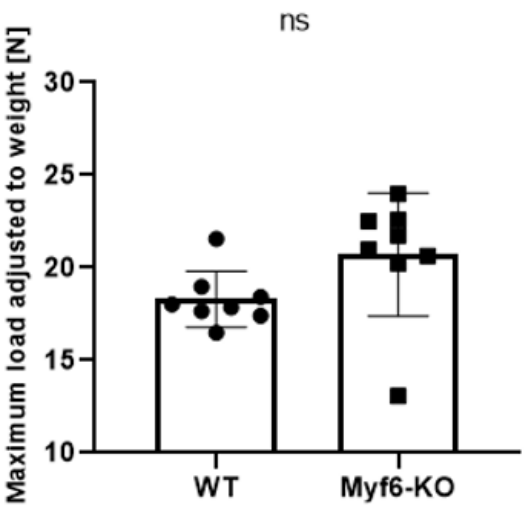
ns
Maximum load adjusted to weight [N]
30
25
20
15
10
WT
Myf6-KO

e

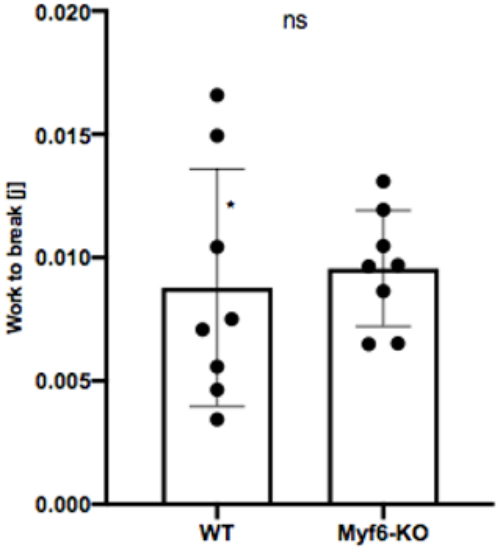
ns
Work to break [j]
0.020
0.015
0.010
0.005
0.000
*
WT
Myf6-KO

f

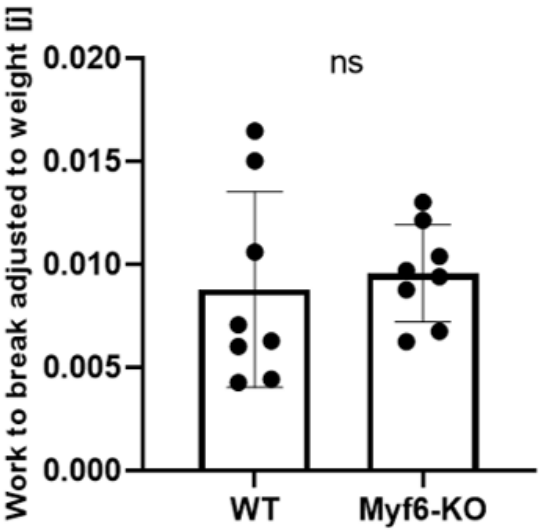
ns
Work to break adjusted to weight [j]
0.020
0.015
0.010
0.005
0.000
WT
Myf6-KO

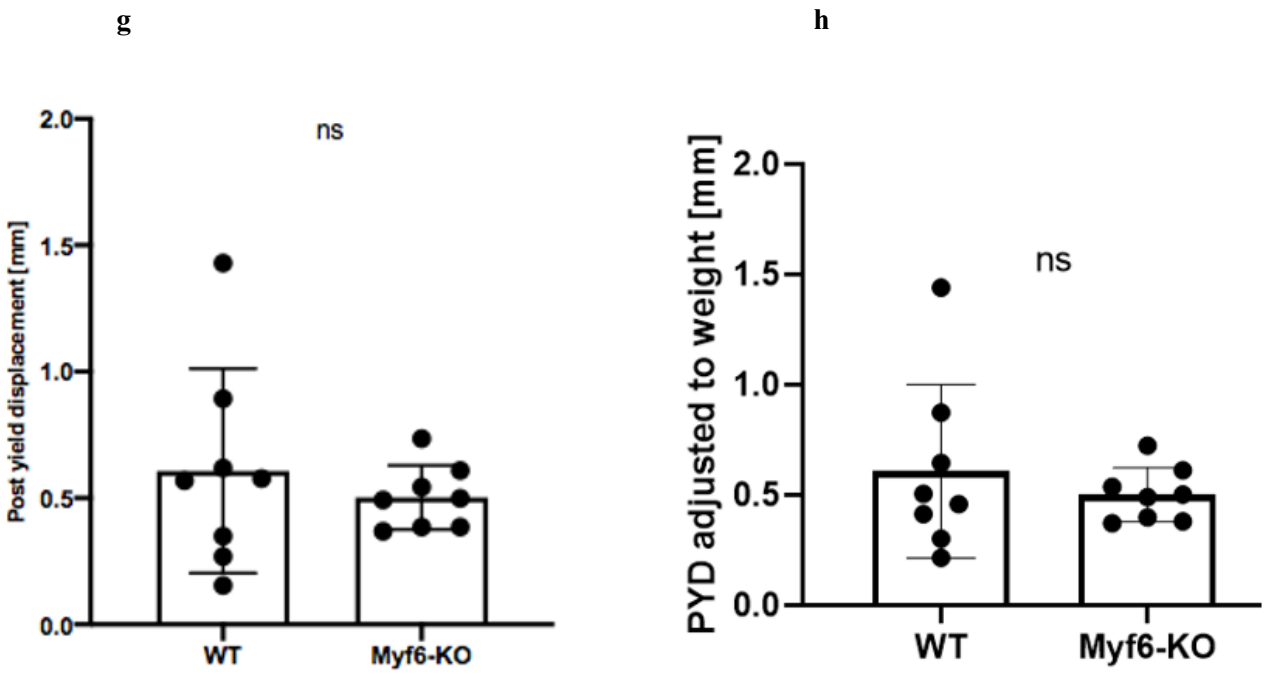

Figure 7: Three-point bending tests results at steady-state. a-b, Stiffness and stiffness adjusted to weight, respectively, **c-d –** Maximum load and maximum load adjusted to weight, respectively, **e-f –** Work to break and work to break adjusted to weight, respectively, **g-h –** Post-yield displacement and post-yield displacement adjusted to weight, respectively. N=8 biological replicates.

3.2.2- Active-state:

The results in **Figure 8** show that there is no difference between the active control and the active *Myf6*-KO cohorts in terms of mechanical performance. Both cohorts seem to be equally strong. This holds true for both the unadjusted and adjusted to body size values.

a

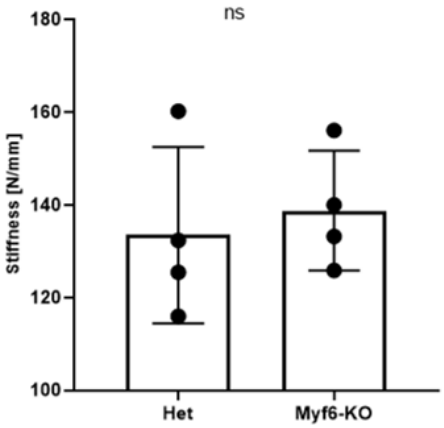
ns
180
160
140
120
100
Stiffness [N/mm]
Het
Myf6-KO

b

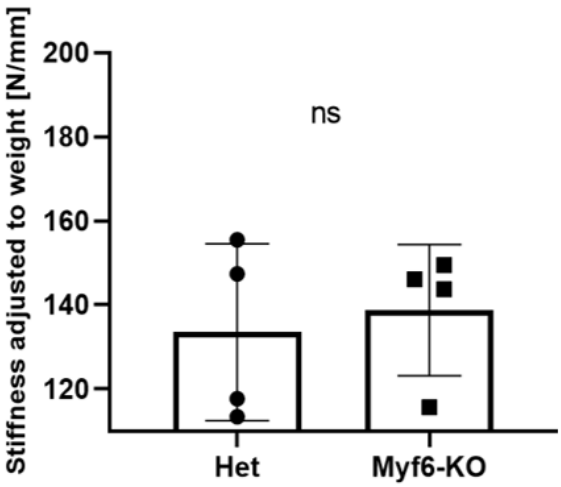
200
180
160
140
120
Stiffness adjusted to weight [N/mm]
ns
Het
Myf6-KO

c

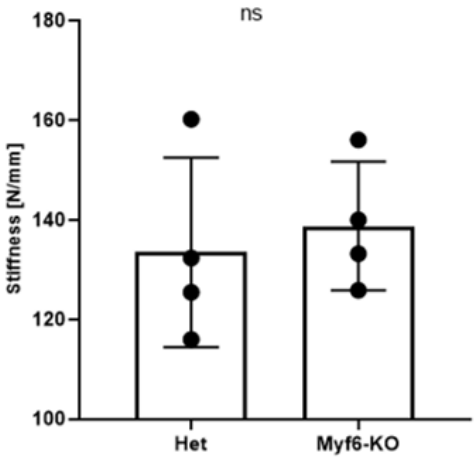
ns
180
160
140
120
100
Stiffness [N/mm]
Het
Myf6-KO

d

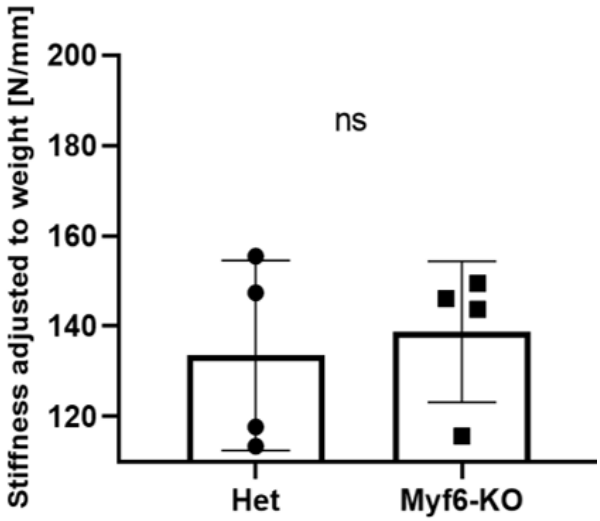
200
180
160
140
120
Stiffness adjusted to weight [N/mm]
ns
Het
Myf6-KO

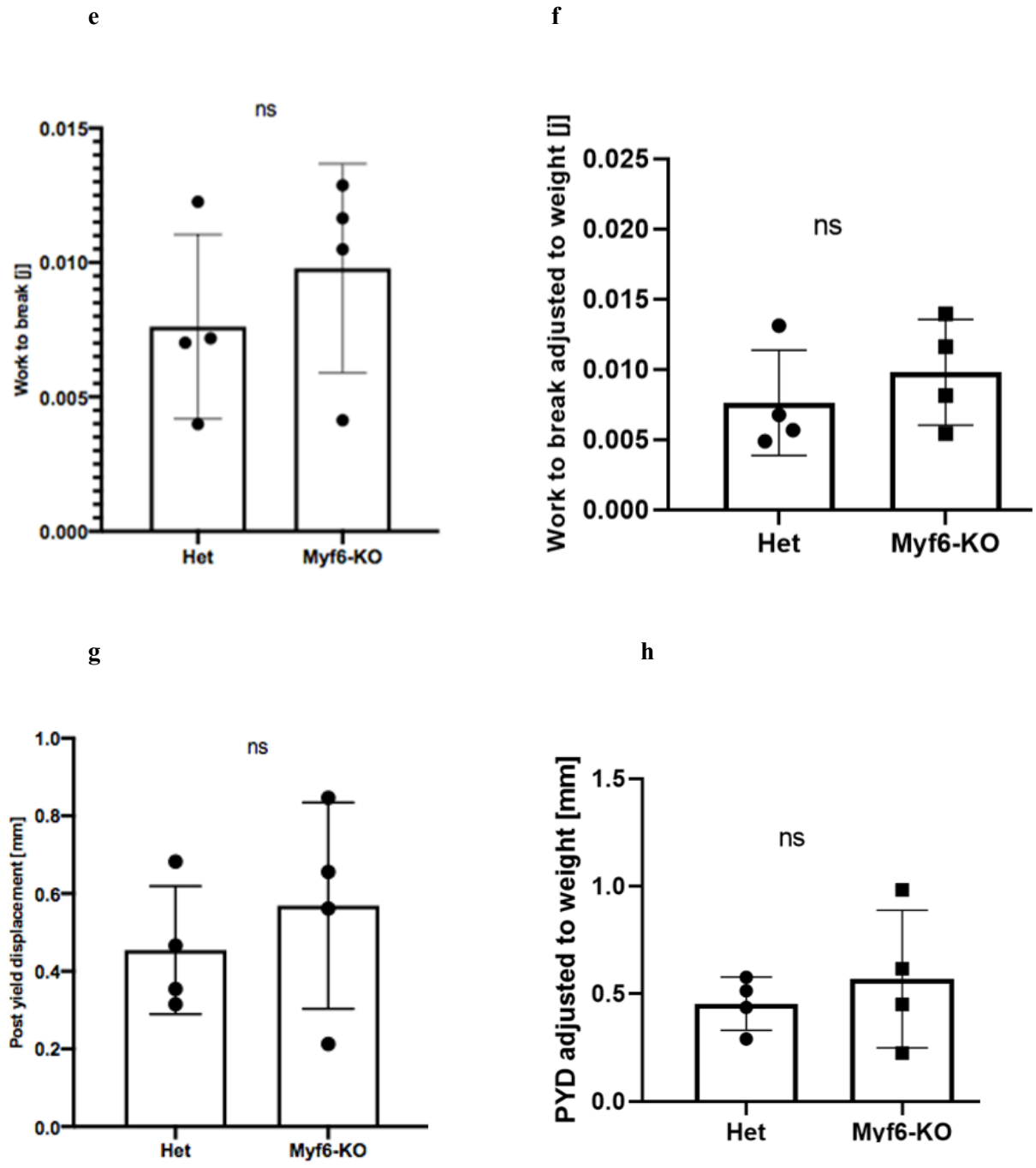

Figure 8: Three-point bending tests results of the active cohort. a-b, Stiffness and stiffness adjusted to weight, respectively, **c-d –** Maximum load and maximum load adjusted to weight, respectively, **e-f –** Work to break and work to break adjusted to weight, respectively, **g-h –** Post-yield displacement and post-yield displacement adjusted to weight, respectively. N=4 biological replicates.

Overall, these results show that there is no difference in the bone morphology and mechanical performance of the wild-type and the *Myf6*-KO cohorts, for both the steady and active condition.

Chapter 4: Discussion

In this study, we investigated the effect of the loss of MYF6, a transcriptional factor expressed in the muscle, on the bones. MYF6 is the principal transcriptional factor that is expressed in the mature myofiber, unlike the other myogenic factors such as MYF5, MyoD, and Myogenin that have a transient expression pattern during myogenic differentiation (Lazure, Blackburn et al. 2019). The genetic loss of *Myf6* in the muscle does not alter myogenic differentiation considering that the mice lacking MYF6 have the same overall muscle structure in terms of size and muscle fibers composition (Lazure, Blackburn et al. 2019). However, the mice lacking MYF6 have a reduced pool of muscle stem cells and decreased myokines in their blood serum (Lazure, Blackburn et al. 2019) (Fig S2, S3).

Considering the extensively documented cross-talk between the muscle and bone, we investigated the role of the MYF6-induced loss of myokines on the bones of the *Myf6*-KO mice. We hypothesised that the loss of MYF6 might have an effect on the morphological and mechanistic properties of the bones, and that such effect would be exacerbated by exercise.

The rationale of this study also involved the possibility that the loss of MYF6-mediated myokines would affect either the osteoblasts, osteocytes, and/ or osteoclasts in the bone. These three types of cells are responsible for the remodelling of the adult bone (Zhang, Wang et al. 2017). While osteoblasts and osteocytes are responsible for the bone formation, osteoclasts are responsible for resorption (Mohamed 2008).

Among the validated myokines that are under the influence of MYF6 is EGF. EGF plays an anabolic role in bone metabolism (Zhang, Tamasi et al. 2011). When EGF receptor (EGFR) was genetically deleted from the preosteoblasts and osteoblasts, both male and female mice had a significant decrease in trabecular bone mass, osteoblast number, femur length, and their associated cortical area and periosteal perimeter (Zhang, Tamasi et al. 2011). Additionally, transgenic mice expressing a modified version of EGF had an accumulation of osteoblasts in the endosteum and periosteum (Chan and Wong 2000)

LIF is also a potential MYF6 targets – although not validated (Lazure, Blackburn et al. 2019). LIF has been reported to stimulate osteoblast differentiation and bone formation (Sims and Johnson 2012) (Lorenzo, Sousa et al. 1990). In Stuve-Wiedemann Syndrome (STWS), LIF deficiency leads to defects in the primary spongiosa and growth plate of the longitudinal bones (Sims and Johnson 2012). LIF is an important cytokine for bone remodelling and the maintenance of a healthy bone mass (Sims and Johnson 2012). Just like LIF, OSM also displays an anabolic role in bone's maintenance (Sims and Quinn 2014) and it also a potential MYF6 target (Lazure, Blackburn et al. 2019).

In the same family of cytokines than LIF, IL-6 and IL-15 (which are also potential targets of MYF6 but are yet to be validated (Lazure, Blackburn et al. 2019)) are also involved in bone resorption (Amarasekara, Yun et al. 2018). Both IL-6 and IL-15 promote osteoclast differentiation and are hence considered osteoclastogenic cytokines (Amarasekara, Yun et al. 2018). Another myokine with a role in bone metabolism that is potentially under the transcriptional control of MYF6 (Lazure, Blackburn et al. 2019) is irisin. Irisin is both secreted by the muscle and is upregulated following exercise (Kim, Wrann et al. 2018). Irisin has been reported to increase the survival of osteocytes and increase the production of sclerostin (Kim, Wrann et al. 2018). Sclerostin is produced by osteocytes and binds to its receptors on osteoblasts (Lewiecki 2014). Sclerostin inhibits bone formation, promoting bone resorption (Lewiecki 2014). Bone formation and bone resorption are the two components of bone remodelling (Mohamed 2008), and a right balance between these two processes is fundamental and crucial for healthy bones.

In our study, we conducted a series of experiments aiming at elucidating the indirect role of MYF6 on the bones. We first used microCT to image the trabecular and cortical area of the tibia of a steady state cohort (N=8), at a great resolution (5µm). The analysis showed no significant difference between the two cohorts in terms of trabecular properties (Fig3). The 2D analysis of the cortical region showed no difference between the two cohorts either (Fig1). Additional volumetric cortical parameters were also not significant (FigS10).

However, there was a significant difference between the two cohorts in terms of cortical porosity (Fig2). Indeed, the *Myf6*-KO cohort had a higher total porosity in the region of interest (ROI) (Fig2c), which also correlated with the percentage occupied by the pores (Fig2b). The pores were mostly located in the endocortical area of the bone, suggesting a potentially higher activity of the osteoclasts in the Myf6-KO mice in that area. Since those

pores were not necessarily all closed, we considered the possibility of a higher vascularization in the *Myf6*-KO bones. It was initially counter-intuitive since those mice lack VEGF-a in their serum (FigS3), which is a growth factor that promotes a higher vascularization in the bone and is a validated target of MYF6 (Hu and Olsen 2016, Filipowska, Tomaszewski et al. 2017) (Lazure, Blackburn et al. 2019). VEGF-a attracts endothelial cells near the bone and controls the function of osteoblasts and osteoclasts (Hu and Olsen 2016) (Filipowska, Tomaszewski et al. 2017). We had no access to a synchrotron radiation microtomography (SR-CT) scanner to visualize the vascular network surrounding the bones in vivo (Lafage-Proust, Roche et al. 2015). However, we performed a fluorescence-activated cell sorting (FACS) (Fig S5) on 4 heterozygous and 4 *Myf6*-KO mice, targeting their adjacent muscle satellite cells ($CD31^-$, $CD11b^-$, $CD45^-$, $sca1^-$, $itga7^+$) (Fig S6) and endothelial cells ($CD31^+$) (Fig S7). There was no significant difference between the two cohorts in terms of satellite cells number nor endothelial cells number.

To assess if the pores made the bone of the *Myf6*-KO mice more brittle or more fragile, we performed a three-point bending test on the unexercised mice (N=8) (Fig 7). There was no significant difference between the performance of the mice, especially in the post-displacement yield (PDY) which is the best indicator to assess the robustness of the bones (Jepsen, Silva et al. 2015). The three-point bending data show that the *Myf6*-KO bones are equally, if not slightly trending towards the stronger side. Further parameters were also not significant for the three-point bending test (Fig S11).

We also looked at the fiber size of the mice, and they were equally large, (FigS4a); supporting the conclusion that the control and *Myf6*-KO mice are equally strong in terms of mechanistic capabilities. Their weight was also not significant (Fig S8), both at the beginning of the swimming test (FigS9a) and after the swimming (Fig S9b).

The same tests were performed on the bones of an active cohort. Four heterozygous and four *Myf6*-KO mice were subjected to an exhaustive swimming test. The mice were forced to swim for 60 minutes a day, 5 days a week. Due to time limitations (only four mice could swim together in the same tank, at the same time) and mice availability (only 8 mice were sex, genotype, and age matched were available), the results reported here are for an N=4. Ideally, the number would be higher.

Two controls and two *Myf6*-KO mice were swimming at the same time to avoid unspecific factors related to the swimming sessions to affect one group and not the other.

The microCT data shows no difference between the two cohorts in terms of cortical or trabecular properties (Fig4-6). The cortical two-dimensional analysis of the tibias shows that they have similar morphologies (Fig 4) while the cortical porosity analysis shows that they have similar porosity (Fig 5). This is in sharp contrast with the steady-state cohort. It is possible that the low number of participating mice is skewing the analysis towards the not-significant side in terms of porosity values. Further mice are needed to draw more robust conclusions in terms of porosity of the active state cohort.

If the number of mice is not the reason behind this discrepancy, it is possible that other factors are produced to overcome the lack of myokines during exercise – which is not the case at rest. Such production might be local to the bones or originating from other organs and tissues. It is possible that those exercise-induced proteins affect the activity of osteoclasts.

The trabecular analysis of the tibias shows no difference in terms of trabecular meshwork components. Both bones are within the same range of trabecular number, trabecular thickness, and trabecular separation (Fig 6).

The bones of both groups are also equally strong following the three-point bending test (Fig 8). The active-state bones of the control and the *Myf6*-KO mice recorded similar performances. The size of their muscle fibers were also within the same range (Fig S4b). One is to note the higher variance in the active heterozygous group, compared to the wild-type group, used for the steady state analysis. While both groups were used as controls in this study, it appears like the heterozygous group is more heterogeneous in terms of parameters values. This might be problematic in terms of data interpretation. It is possible that the Myf6-heterozygous group has an inconsistent expression of MYF6, which might explain the wider range of values. While the heterozygous mice were successfully used as controls before (Lazure, Blackburn et al. 2019), it is a possibility that we cannot rule out. For bone related experiments in the future, wild-type mice are better controls.

Together, these findings are overall consistent in supporting the statement that the lack of MYF6 does not significantly impact bone's health. At both steady and active state, the bones have the same trabecular architecture, mostly the same cortical properties, and the same mechanistic performance. At steady-state, the porosity of the *Myf6*-KO mice was more important. This is something that can be investigated further.

The fact that the myokines loss does not dramatically affect bone remodelling might be explained by the ubiquitous expression of some cytokines. (Leonard‡ 2002). Although the myokines are called myokines because they are produced in the muscle, they are not exclusive to the muscle (Kovanen and Leonard 2004, Akdis, Burgler et al. 2011). Most of the aforementioned myokines are also produced locally, by the bone cells. This means that even if the myokines are decreased in the serum, the local production of those myokines might be more relevant to the bones than the ones produced elsewhere in the body.

VEGF-a for example is produced by both the hypertrophic chondrocytes and the perichondrial osteolineage cells to recruit blood vessels in the perichondrium and allow for the osteoblast to differentiate (Duan, Murata et al. 2015). LIF is produced by the primary mesenchymal stell cells and bone marrow stromal cells, which are the precursors of the osteoblasts and osteoclasts (Sims and Johnson 2012). LIF is also produced in the bone-joint microenvironment, explaining its involvement in the inflammation of those areas (Sims and Johnson 2012). OSM, which stimulates bone accrual (Sims and Quinn 2014), is also produced by the same cells that LIF (Sims and Quinn 2014). IL-6 is produced by osteoblasts (Tseng, Lu et al. 2010) and promotes osteoclastogenesis (Harmer, Falank et al. 2019). IL-6 is also stored in the bone matrix once its secreted by inflammatory cells naturally present in the bone (Harmer, Falank et al. 2019). IL-15 on the other hand is secreted by the Chimeric antigen receptor (CAR) cells in the bone marrow, which gives the bone a direct access to this interleukin (Cui, Hara et al. 2014).

Another potential explanation is that multiple pathways exist to activate or inhibit the osteoblasts (Rutkovskiy, Stensløkken et al. 2016) (Parvizi and Kim 2010) and osteoclasts (Lorenzo 2017). If one myokine is not present, the same activation or inhibition can still be achieved by another cytokine, interleukin, or peptide (Lorenzo 2017) (Boyle, Simonet et al. 2003). This functional redundancy is important evolutionary speaking since it allows the organisms to have alternative ways when one no longer functions optimally (Kafri, Levy et al. 2006, Bedner, Steinhäuser et al. 2012).

Chapter 5: Conclusion and Future Directions

In summary, the muscle is in constant cross-talk with the peripheric organs by either exerting a paracrine or an endocrine function. This systematic effect is enhanced by exercise. In multicellular organisms, different roles rose for each organ and tissue; and constant and efficient communication between them is crucial (Yamada and Katagiri 2007) (Plauth, Raible et al. 1993). Different cytokines, interleukins, hormones, and peptides took on the role of mediators, not only from the muscle to other organs (He, Tian et al. 2018) (Pedersen and Febbraio 2008), but from other organs to the muscle as well (Shimizu, Maruyama et al. 2015). When exercising, our need for energy and oxygen expenditure increase, and so 'updating' the peripheral organs on the current condition has a paramount importance in adapting, especially during flight or fight situations (Huber, Petzold et al. 2007).

In this study, we investigated the role of Myf6-mediated cross-talk between muscle and bone. MYF6 has a maintained uniform expression in the mature fibers of the muscle (Lazure, Blackburn et al. 2019) and was shown to be responsible for the expression of a vast array of myokines, especially EGF and VEGF-a which are validated targets (Lazure, Blackburn et al. 2019). Here we show that the lack of MYF6 in the muscle, and consequently the serum depletion of the myokines that are under its transcriptional control, have no significant detrimental effect on bone's health.

At both steady and active state, the bones of the control and *Myf6*-KO mice have similar mechanistic performances and overall morphological properties. The porosity at steady state was significant between the control and the *Myf6*-KO group. A tartrate-resistant acid phosphate (TRAP) staining can be performed to investigate the osteoclastic activity further, alongside a dynamic histomorphometry.

It would also be informative to measure some of the bone remodelling markers in the serum of the mice using ELISA kits: C-telopeptide fragments of type II collagen (CTXII) for bone resorption and procollagen I N - Terminal Propeptide (PINP) for bone formation.

From a clinical perspective, even though this study showed quite conclusively that there is no *functional* detrimental effect on the bones when MYF6 is missing, the *Myf6*-KO mice can still be an exercise model, in the context of a different organ. The bone was the only tissue to be investigated here; it is possible that the loss of myokines negatively influences another organ.

In the FACS plot (Figure S5), we can see that the immune cells (white) are more abundant in the *Myf6*-KO mice. It is possible that the immune cells trigger an inflammatory response in the joints in the absence of the myokines. This can also be investigated further, especially since myokines such as IL-6 and LIF were reported to have anti-inflammatory properties when secreted by the muscle (Brandt and Pedersen 2010, Hunt, Upadhyay et al. 2013, Welc and Clanton 2013, Davis, Collier et al. 2018).

Another point that needs to be addressed in this study is the fact that even if myokines answer some of the questions related to adaptation to exercise and movement, there are still many challenges to overcome before reaching final and conclusive statements about their exact role. The very definition of myokine is problematic. A myokine is generally defined as a protein or peptide produced by the muscle (Pedersen and Febbraio 2008). For many studies, myokines were identified as such by RNA-seq of the *whole* muscle (Lin, Chang et al. 2018) (Pourteymour, Eckardt et al. 2017). The issue is that 'whole muscle' has connective tissue, endothelial cells, and immune cells associated with it (Mukund and Subramaniam 2020). The exact provenance of these myokines is hence problematic. This can be overcome by performing single-cell RNA seq, which was performed recently (Rubenstein, Smith et al. 2020).

The source of the circulating myokines has another layer of complexity since most of them are also produced by peripheral organs altogether (Leal, Lopes et al. 2018). It is hence difficult to determine the real contribution of muscle-derived myokines alone, as it was proven true in this very study.

Further research is needed to elucidate the role of myokines, especially the ones that are poorly understood and linked to contradicting conclusions. While the big picture is drawn, the details are still very much missing. Transgenic mice for *Myf6* are potentially *in vivo* exercise models that may allow us to better understand the systematic effect of exercise on peripheral organs. Bones were investigated here with negative results, but other organs and tissues are still potential targets.

Chapter 6: References

Muscle as a Secretory Organ. Comprehensive Physiology**:** 1337-1362.

(1997). "Guidelines for school and community programs to promote lifelong physical activity among young people. Centers for Disease Control and Prevention." MMWR Recomm Rep **46**(Rr-6): 1-36.

(1998). "Additional evidence that walking has health benefits." Mayo Clin Health Lett **16**(5): 4.

(1998). "American College of Sports Medicine Position Stand. Exercise and physical activity for older adults." Med Sci Sports Exerc **30**(6): 992-1008.

(1998). "American College of Sports Medicine Position Stand. The recommended quantity and quality of exercise for developing and maintaining cardiorespiratory and muscular fitness, and flexibility in healthy adults." Med Sci Sports Exerc **30**(6): 975-991.

Abou Neel, E. A., A. Aljabo, A. Strange, S. Ibrahim, M. Coathup, A. M. Young, L. Bozec and V. Mudera (2016). "Demineralization-remineralization dynamics in teeth and bone." International journal of nanomedicine **11**: 4743-4763.

Adebanjo, O. A., B. S. Moonga, T. Yamate, L. Sun, C. Minkin, E. Abe and M. Zaidi (1998). "Mode of action of interleukin-6 on mature osteoclasts. Novel interactions with extracellular Ca2+ sensing in the regulation of osteoclastic bone resorption." The Journal of cell biology **142**(5): 1347-1356.

Akdis, M., S. Burgler, R. Crameri, T. Eiwegger, H. Fujita, E. Gomez, S. Klunker, N. Meyer, L. O'Mahony, O. Palomares, C. Rhyner, N. Ouaked, A. Schaffartzik, W. Van De Veen, S. Zeller, M. Zimmermann and C. A. Akdis (2011). "Interleukins, from 1 to 37, and interferon-γ: receptors, functions, and roles in diseases." J Allergy Clin Immunol **127**(3): 701-721.e701-770.

Allbrook, D. B., M. F. Han and A. E. Hellmuth (1971). "Population of muscle satellite cells in relation to age and mitotic activity." Pathology **3**(3): 223-243.

Amarasekara, D. S., H. Yun, S. Kim, N. Lee, H. Kim and J. Rho (2018). "Regulation of Osteoclast Differentiation by Cytokine Networks." Immune network **18**(1): e8-e8.

Asfour, H. A., M. Z. Allouh and R. S. Said (2018). "Myogenic regulatory factors: The orchestrators of myogenesis after 30 years of discovery." Experimental biology and medicine (Maywood, N.J.) **243**(2): 118-128.

Asfour, H. A., M. Z. Allouh and R. S. Said (2018). "Myogenic regulatory factors: The orchestrators of myogenesis after 30 years of discovery." Exp Biol Med (Maywood) **243**(2): 118-128.

Baghdadi, M. B. and S. Tajbakhsh (2018). "Regulation and phylogeny of skeletal muscle regeneration." Developmental Biology **433**(2): 200-209.

Baldwin, K. M. and F. Haddad (2019). Chapter 16 - The Evolution of Skeletal Muscle Plasticity in Response to Physical Activity and Inactivity. Muscle and Exercise Physiology. J. A. Zoladz, Academic Press**:** 347-377.

Bareja, A. and A. N. Billin (2013). "Satellite cell therapy – from mice to men." Skeletal Muscle **3**(1): 2.

Barhoumi, T., M. Briet, D. A. Kasal, J. C. Fraulob-Aquino, N. Idris-Khodja, P. Laurant, P. Paradis and E. L. Schiffrin (2014). "Erythropoietin-induced hypertension and vascular injury in mice overexpressing human endothelin-1: exercise attenuated hypertension, oxidative stress, inflammation and immune response." J Hypertens **32**(4): 784-794.

Bedner, P., C. Steinhäuser and M. Theis (2012). "Functional redundancy and compensation among members of gap junction protein families?" Biochimica et Biophysica Acta (BBA) - Biomembranes **1818**(8): 1971-1984.

Benedetti, M. G., G. Furlini, A. Zati and G. Letizia Mauro (2018). "The Effectiveness of Physical Exercise on Bone Density in Osteoporotic Patients." BioMed research international **2018**: 4840531-4840531.

Bentzinger, C. F., Y. X. Wang and M. A. Rudnicki (2012). "Building muscle: molecular regulation of myogenesis." Cold Spring Harbor perspectives in biology **4**(2): a008342.

Blanchard, F., L. Duplomb, M. Baud'huin and B. Brounais (2009). "The dual role of IL-6-type cytokines on bone remodeling and bone tumors." Cytokine & Growth Factor Reviews **20**(1): 19-28.

Bonaiuti, D., B. Shea, R. Iovine, S. Negrini, V. Robinson, H. C. Kemper, G. Wells, P. Tugwell and A. Cranney (2002). "Exercise for preventing and treating osteoporosis in postmenopausal women." Cochrane Database Syst Rev(3): Cd000333.

Bortoluzzi, S., P. Scannapieco, A. Cestaro, G. A. Danieli and S. Schiaffino (2006). "Computational reconstruction of the human skeletal muscle secretome." Proteins: Structure, Function, and Bioinformatics **62**(3): 776-792.

Boskey, A. L. and R. Coleman (2010). "Aging and bone." Journal of dental research **89**(12): 1333-1348.

Bouxsein, M. L., S. K. Boyd, B. A. Christiansen, R. E. Guldberg, K. J. Jepsen and R. Müller (2010). "Guidelines for assessment of bone microstructure in rodents using micro-computed tomography." J Bone Miner Res **25**(7): 1468-1486.

Boyle, W. J., W. S. Simonet and D. L. Lacey (2003). "Osteoclast differentiation and activation." Nature **423**(6937): 337-342.

Brandt, C. and B. K. Pedersen (2010). "The Role of Exercise-Induced Myokines in Muscle Homeostasis and the Defense against Chronic Diseases." Journal of Biomedicine and Biotechnology **2010**: 520258.

Braun, T. and H. H. Arnold (1995). "Inactivation of Myf-6 and Myf-5 genes in mice leads to alterations in skeletal muscle development." The EMBO Journal **14**(6): 1176-1186.

Braun, T., E. Bober, B. Winter, N. Rosenthal and H. H. Arnold (1990). "Myf-6, a new member of the human gene family of myogenic determination factors: evidence for a gene cluster on chromosome 12." Embo j **9**(3): 821-831.

Brotto, M. and M. L. Johnson (2014). "Endocrine crosstalk between muscle and bone." Curr Osteoporos Rep **12**(2): 135-141.

Caldow, M. K., E. E. Thomas, M. J. Dale, G. R. Tomkinson, J. D. Buckley and D. Cameron-Smith (2015). "Early myogenic responses to acute exercise before and after resistance training in young men." Physiological reports **3**(9): e12511.

Capulli, M., R. Paone and N. Rucci (2014). "Osteoblast and osteocyte: Games without frontiers." Archives of Biochemistry and Biophysics **561**: 3-12.

Catoire, M., M. Mensink, E. Kalkhoven, P. Schrauwen and S. Kersten (2014). "Identification of human exercise-induced myokines using secretome analysis." Physiol Genomics **46**(7): 256-267.

Chan, S. Y. and R. W. Wong (2000). "Expression of epidermal growth factor in transgenic mice causes growth retardation." J Biol Chem **275**(49): 38693-38698.

Ciano, M., G. Mantellato, M. Connolly, M. Paul-Clark, S. Willis-Owen, M. F. Moffatt, W. O. C. M. Cookson, J. A. Mitchell, M. I. Polkey, S. M. Hughes, P. R. Kemp and S. A. Natanek (2019). "EGF receptor (EGFR) inhibition promotes a slow-twitch oxidative, over a fast-twitch, muscle phenotype." Scientific reports **9**(1): 9218-9218.

Clarke, B. (2008). "Normal bone anatomy and physiology." Clinical journal of the American Society of Nephrology : CJASN **3 Suppl 3**(Suppl 3): S131-S139.

Colaianni, G., C. Cuscito, T. Mongelli, A. Oranger, G. Mori, G. Brunetti, S. Colucci, S. Cinti and M. Grano (2014). "Irisin enhances osteoblast differentiation in vitro." International journal of endocrinology **2014**: 902186-902186.

Colaianni, G., C. Cuscito, T. Mongelli, P. Pignataro, C. Buccoliero, P. Liu, P. Lu, L. Sartini, M. Di Comite, G. Mori, A. Di Benedetto, G. Brunetti, T. Yuen, L. Sun, J. E. Reseland, S. Colucci, M. I. New, M. Zaidi, S. Cinti and M. Grano (2015). "The myokine irisin increases cortical bone mass." Proceedings of the National Academy of Sciences of the United States of America **112**(39): 12157-12162.

Colaianni, G. and M. Grano (2015). "Role of Irisin on the bone-muscle functional unit." BoneKEy reports **4**: 765-765.

Colaianni, G., T. Mongelli, S. Colucci, S. Cinti and M. Grano (2016). "Crosstalk Between Muscle and Bone Via the Muscle-Myokine Irisin." Current Osteoporosis Reports **14**(4): 132-137.

Colaianni, G., L. Sanesi, G. Storlino, G. Brunetti, S. Colucci and M. Grano (2019). "Irisin and Bone: From Preclinical Studies to the Evaluation of Its Circulating Levels in Different Populations of Human Subjects." Cells **8**(5): 451.

Cooper, B. (2011). "The origins of bone marrow as the seedbed of our blood: from antiquity to the time of Osler." Proceedings (Baylor University. Medical Center) **24**(2): 115-118.

Cui, G., T. Hara, S. Simmons, K. Wagatsuma, A. Abe, H. Miyachi, S. Kitano, M. Ishii, S. Tani-ichi and K. Ikuta (2014). "Characterization of the IL-15 niche in primary and secondary lymphoid organs in vivo." Proceedings of the National Academy of Sciences **111**(5): 1915.

D'Lugos, A. C., S. H. Patel, J. C. Ormsby, D. P. Curtis, C. S. Fry, C. C. Carroll and J. M. Dickinson (2018). "Prior acetaminophen consumption impacts the early adaptive cellular response of human skeletal muscle to resistance exercise." Journal of Applied Physiology **124**(4): 1012-1024.

Davis, S. M., L. A. Collier, E. D. Winford, C. C. Leonardo, C. T. Ajmo, E. A. Foran, T. J. Kopper, J. C. Gensel and K. R. Pennypacker (2018). "Leukemia inhibitory factor modulates the peripheral immune response in a rat model of emergent large vessel occlusion." Journal of Neuroinflammation **15**(1): 288.

Driscoll, P. (2006). "Gray's Anatomy, 39th Edition." Emergency Medicine Journal : EMJ **23**(6): 492-492.

Du, C., Y.-Q. Jin, J.-J. Qi, Z.-X. Ji, S.-Y. Li, G.-S. An, H.-T. Jia and J.-H. Ni (2012). "Effects of myogenin on expression of late muscle genes through MyoD-dependent chromatin remodeling ability of myogenin." Molecules and Cells **34**(2): 133-142.

Duan, X., Y. Murata, Y. Liu, C. Nicolae, B. R. Olsen and A. D. Berendsen (2015). "Vegfa regulates perichondrial vascularity and osteoblast differentiation in bone development." Development **142**(11): 1984-1991.

Fan, C.-M., L. Li, M. E. Rozo and C. Lepper (2012). "Making skeletal muscle from progenitor and stem cells: development versus regeneration." WIREs Developmental Biology **1**(3): 315-327.
Febbraio, M. A. and B. K. Pedersen (2002). "Muscle-derived interleukin-6: mechanisms for activation and possible biological roles." Faseb j **16**(11): 1335-1347.
Filipowska, J., K. A. Tomaszewski, Ł. Niedźwiedzki, J. A. Walocha and T. Niedźwiedzki (2017). "The role of vasculature in bone development, regeneration and proper systemic functioning." Angiogenesis **20**(3): 291-302.
Friedland, R. P., T. Fritsch, K. A. Smyth, E. Koss, A. J. Lerner, C. H. Chen, G. J. Petot and S. M. Debanne (2001). "Patients with Alzheimer's disease have reduced activities in midlife compared with healthy control-group members." Proc Natl Acad Sci U S A **98**(6): 3440-3445.
Friedrichs, M., F. Wirsdöerfer, S. B. Flohé, S. Schneider, M. Wuelling and A. Vortkamp (2011). "BMP signaling balances proliferation and differentiation of muscle satellite cell descendants." BMC Cell Biology **12**(1): 26.
Füchtbauer, E. M. and H. Westphal (1992). "MyoD and myogenin are coexpressed in regenerating skeletal muscle of the mouse." Dev Dyn **193**(1): 34-39.
Funk, J. R., J. R. Kerrigan and J. R. Crandall (2004). "Dynamic bending tolerance and elastic-plastic material properties of the human femur." Annual proceedings. Association for the Advancement of Automotive Medicine **48**: 215-233.
Gillies, A. R. and R. L. Lieber (2011). "Structure and function of the skeletal muscle extracellular matrix." Muscle & nerve **44**(3): 318-331.
Goldstein, M. S. (1961). "Humoral nature of the hypoglycemic factor of muscular work." Diabetes **10**: 232-234.
Gomez-Bruton, A., A. Gonzalez-Aguero, A. Gomez-Cabello, A. Matute-Llorente, J. A. Casajus and G. Vicente-Rodriguez (2016). "Swimming and bone: Is low bone mass due to hypogravity alone or does other physical activity influence it?" Osteoporos Int **27**(5): 1785-1793.
Gorgens, S. W., K. Eckardt, J. Jensen, C. A. Drevon and J. Eckel (2015). "Exercise and Regulation of Adipokine and Myokine Production." Prog Mol Biol Transl Sci **135**: 313-336.
Haldar, M., G. Karan, P. Tvrdik and M. R. Capecchi (2008). "Two Cell Lineages, myf5 and myf5-Independent, Participate in Mouse Skeletal Myogenesis." Developmental Cell **14**(3): 437-445.

Hamrick, M. W., P. L. McNeil and S. L. Patterson (2010). "Role of muscle-derived growth factors in bone formation." Journal of musculoskeletal & neuronal interactions **10**(1): 64-70.
Harmer, D., C. Falank and M. R. Reagan (2019). "Interleukin-6 Interweaves the Bone Marrow Microenvironment, Bone Loss, and Multiple Myeloma." Frontiers in endocrinology **9**: 788-788.
He, Z., Y. Tian, P. L. Valenzuela, C. Huang, J. Zhao, P. Hong, Z. He, S. Yin and A. Lucia (2018). "Myokine Response to High-Intensity Interval vs. Resistance Exercise: An Individual Approach." Frontiers in Physiology **9**(1735).
Hong, A. R. and S. W. Kim (2018). "Effects of Resistance Exercise on Bone Health." Endocrinology and metabolism (Seoul, Korea) **33**(4): 435-444.
Hu, K. and B. R. Olsen (2016). "Osteoblast-derived VEGF regulates osteoblast differentiation and bone formation during bone repair." The Journal of Clinical Investigation **126**(2): 509-526.
Huber, K., J. Petzold, C. Rehfeldt, K. Ender and I. Fiedler (2007). "Muscle energy metabolism: structural and functional features in different types of porcine striated muscles." J Muscle Res Cell Motil **28**(4-5): 249-258.
Huelke, D. F. (1998). "An Overview of Anatomical Considerations of Infants and Children in the Adult World of Automobile Safety Design." Annual Proceedings / Association for the Advancement of Automotive Medicine **42**: 93-113.
Hunt, L. C., A. Upadhyay, J. A. Jazayeri, E. M. Tudor and J. D. White (2013). "An anti-inflammatory role for leukemia inhibitory factor receptor signaling in regenerating skeletal muscle." Histochem Cell Biol **139**(1): 13-34.
Jepsen, K. J. (2009). "Systems analysis of bone." Wiley interdisciplinary reviews. Systems biology and medicine **1**(1): 73-88.
Jepsen, K. J., M. J. Silva, D. Vashishth, X. E. Guo and M. C. van der Meulen (2015). "Establishing biomechanical mechanisms in mouse models: practical guidelines for systematically evaluating phenotypic changes in the diaphyses of long bones." J Bone Miner Res **30**(6): 951-966.
Kafri, R., M. Levy and Y. Pilpel (2006). "The regulatory utilization of genetic redundancy through responsive backup circuits." Proceedings of the National Academy of Sciences **103**(31): 11653.
Kaji, H. (2016). "Effects of myokines on bone." BoneKEy reports **5**: 826-826.
Kalenderer Ö., T. A. (2016). Bone., Springer, Cham.

Keller, C., A. Steensberg, H. Pilegaard, T. Osada, B. Saltin, B. K. Pedersen and P. D. Neufer (2001). "Transcriptional activation of the IL-6 gene in human contracting skeletal muscle: influence of muscle glycogen content." Faseb j **15**(14): 2748-2750.

Kersh, M. E., P. K. Zysset, D. H. Pahr, U. Wolfram, D. Larsson and M. G. Pandy (2013). "Measurement of structural anisotropy in femoral trabecular bone using clinical-resolution CT images." J Biomech **46**(15): 2659-2666.

Kim, H., C. D. Wrann, M. Jedrychowski, S. Vidoni, Y. Kitase, K. Nagano, C. Zhou, J. Chou, V. A. Parkman, S. J. Novick, T. S. Strutzenberg, B. D. Pascal, P. T. Le, D. J. Brooks, A. M. Roche, K. K. Gerber, L. Mattheis, W. Chen, H. Tu, M. L. Bouxsein, P. R. Griffin, R. Baron, C. J. Rosen, L. F. Bonewald and B. M. Spiegelman (2018). "Irisin Mediates Effects on Bone and Fat via αV Integrin Receptors." Cell **175**(7): 1756-1768.e1717.

Kovanen, P. E. and W. J. Leonard (2004). "Cytokines and immunodeficiency diseases: critical roles of the gamma(c)-dependent cytokines interleukins 2, 4, 7, 9, 15, and 21, and their signaling pathways." Immunol Rev **202**: 67-83.

Kuang, S., K. Kuroda, F. Le Grand and M. A. Rudnicki (2007). "Asymmetric Self-Renewal and Commitment of Satellite Stem Cells in Muscle." Cell **129**(5): 999-1010.

Lafage-Proust, M.-H., B. Roche, M. Langer, D. Cleret, A. Vanden Bossche, T. Olivier and L. Vico (2015). "Assessment of bone vascularization and its role in bone remodeling." BoneKEy reports **4**: 662-662.

Lazure, F., D. M. Blackburn, N. Karam, K. Sahinyan, A. Sharanek, D. Nguyen, A. H. Corchado, C. Lepper, H. S. Najafabadi, T. J. Perkins, A. Jahani-Asl and V. Soleimani (2019). "Myf6/MRF4 is a Myogenic Niche Regulator Required for the Maintenance of the Muscle Stem Cell Pool." bioRxiv: 691386.

Le Grand, F. and M. A. Rudnicki (2007). "Skeletal muscle satellite cells and adult myogenesis." Current Opinion in Cell Biology **19**(6): 628-633.

Leal, L. G., M. A. Lopes and M. L. Batista, Jr. (2018). "Physical Exercise-Induced Myokines and Muscle-Adipose Tissue Crosstalk: A Review of Current Knowledge and the Implications for Health and Metabolic Diseases." Frontiers in physiology **9**: 1307-1307.

Leonard‡, K. O. a. W. J. (2002). "Cytokine and Cytokine Receptor Pleiotropy and Redundancy*." The journal of biological chemistry **277**.

Levy, J. B., C. Schindler, R. Raz, D. E. Levy, R. Baron and M. C. Horowitz (1996). "Activation of the JAK-STAT signal transduction pathway by oncostatin-M cultured human and mouse osteoblastic cells." Endocrinology **137**(4): 1159-1165.

Lewiecki, E. M. (2014). "Role of sclerostin in bone and cartilage and its potential as a therapeutic target in bone diseases." Therapeutic advances in musculoskeletal disease **6**(2): 48-57.
Lin, I. H., J.-L. Chang, K. Hua, W.-C. Huang, M.-T. Hsu and Y.-F. Chen (2018). "Skeletal muscle in aged mice reveals extensive transformation of muscle gene expression." BMC Genetics **19**(1): 55.
Lorenzo, J. (2017). "The many ways of osteoclast activation." The Journal of clinical investigation **127**(7): 2530-2532.
Lorenzo, J. A., S. L. Sousa and C. L. Leahy (1990). "Leukemia inhibitory factor (LIF) inhibits basal bone resorption in fetal rat long bone cultures." Cytokine **2**(4): 266-271.
Maurel, D. B., K. Jähn and N. Lara-Castillo (2017). "Muscle-Bone Crosstalk: Emerging Opportunities for Novel Therapeutic Approaches to Treat Musculoskeletal Pathologies." Biomedicines **5**(4): 62.
Milewska, M., T. Domoradzki, A. Majewska, M. Blaszczyk, M. Gajewska, M. Hulanicka and K. Grzelkowska-Kowalczyk (2019). "Interleukin-6 affects pacsin3, ephrinA4 expression and cytoskeletal proteins in differentiating primary skeletal myoblasts through transcriptional and post-transcriptional mechanisms." Cell Tissue Res.
Mohamed, A. M. (2008). "An overview of bone cells and their regulating factors of differentiation." The Malaysian journal of medical sciences : MJMS **15**(1): 4-12.
Moretti, I., S. Ciciliot, K. A. Dyar, R. Abraham, M. Murgia, L. Agatea, T. Akimoto, S. Bicciato, M. Forcato, P. Pierre, N. H. Uhlenhaut, P. W. J. Rigby, J. J. Carvajal, B. Blaauw, E. Calabria and S. Schiaffino (2016). "MRF4 negatively regulates adult skeletal muscle growth by repressing MEF2 activity." Nature Communications **7**(1): 12397.
Mourikis, P. and F. Relaix (2016). "Activated Muscle Satellite Cells Chase Ghosts." Cell Stem Cell **18**(2): 160-162.
Mukund, K. and S. Subramaniam (2020). "Skeletal muscle: A review of molecular structure and function, in health and disease." Wiley interdisciplinary reviews. Systems biology and medicine **12**(1): e1462-e1462.
Neunhäuserer, D., M. Zebedin, M. Obermoser, G. Moser, M. Tauber, J. Niebauer, H. Resch and S. Galler (2011). "Human skeletal muscle: transition between fast and slow fibre types." Pflugers Arch **461**(5): 537-543.
Parvizi, J. and G. K. Kim (2010). Chapter 160 - Osteoblasts. High Yield Orthopaedics. J. Parvizi and G. K. Kim. Philadelphia, W.B. Saunders**:** 331-332.

Pedersen, B. K. and M. A. Febbraio (2008). "Muscle as an endocrine organ: focus on muscle-derived interleukin-6." Physiol Rev **88**(4): 1379-1406.
Pedersen, B. K., A. Steensberg, C. Fischer, C. Keller, P. Keller, P. Plomgaard, M. Febbraio and B. Saltin (2003). "Searching for the exercise factor: is IL-6 a candidate?" J Muscle Res Cell Motil **24**(2-3): 113-119.
Plauth, M., A. Raible, M. Gregor and F. Hartmann (1993). "Inter-organ communication between intestine and liver in vivo and in vitro." Seminars in Cell Biology **4**(3): 231-237.
Pourteymour, S., K. Eckardt, T. Holen, T. Langleite, S. Lee, J. Jensen, K. I. Birkeland, C. A. Drevon and M. Hjorth (2017). "Global mRNA sequencing of human skeletal muscle: Search for novel exercise-regulated myokines." Molecular metabolism **6**(4): 352-365.
Pourteymour, S., K. Eckardt, T. Holen, T. Langleite, S. Lee, J. Jensen, K. I. Birkeland, C. A. Drevon and M. Hjorth (2017). "Global mRNA sequencing of human skeletal muscle: Search for novel exercise-regulated myokines." Mol Metab **6**(4): 352-365.
Relaix, F., D. Rocancourt, A. Mansouri and M. Buckingham (2005). "A Pax3/Pax7-dependent population of skeletal muscle progenitor cells." Nature **435**(7044): 948-953.
Rubenstein, A. B., G. R. Smith, U. Raue, G. Begue, K. Minchev, F. Ruf-Zamojski, V. D. Nair, X. Wang, L. Zhou, E. Zaslavsky, T. A. Trappe, S. Trappe and S. C. Sealfon (2020). "Single-cell transcriptional profiles in human skeletal muscle." Scientific Reports **10**(1): 229.
Rutkovskiy, A., K.-O. Stensløkken and I. J. Vaage (2016). "Osteoblast Differentiation at a Glance." Medical science monitor basic research **22**: 95-106.
Salmon, P. L., C. Ohlsson, S. J. Shefelbine and M. Doube (2015). "Structure Model Index Does Not Measure Rods and Plates in Trabecular Bone." Frontiers in endocrinology **6**: 162-162.
Seale, P., L. A. Sabourin, A. Girgis-Gabardo, A. Mansouri, P. Gruss and M. A. Rudnicki (2000). "Pax7 Is Required for the Specification of Myogenic Satellite Cells." Cell **102**(6): 777-786.
Shefer, G., D. P. Van de Mark, J. B. Richardson and Z. Yablonka-Reuveni (2006). "Satellite-cell pool size does matter: defining the myogenic potency of aging skeletal muscle." Developmental biology **294**(1): 50-66.
Shen, Y. and S. K. Nilsson (2012). "Bone, microenvironment and hematopoiesis." Curr Opin Hematol **19**(4): 250-255.
Shimizu, N., T. Maruyama, N. Yoshikawa, R. Matsumiya, Y. Ma, N. Ito, Y. Tasaka, A. Kuribara-Souta, K. Miyata, Y. Oike, S. Berger, G. Schütz, S. i. Takeda and H. Tanaka

(2015). "A muscle-liver-fat signalling axis is essential for central control of adaptive adipose remodelling." Nature Communications **6**(1): 6693.
Sims, N. A. and R. W. Johnson (2012). "Leukemia inhibitory factor: A paracrine mediator of bone metabolism." Growth Factors **30**(2): 76-87.
Sims, N. A. and J. M. W. Quinn (2014). "Osteoimmunology: oncostatin M as a pleiotropic regulator of bone formation and resorption in health and disease." BoneKEy reports **3**: 527-527.
Singh, B., G. Carpenter and R. J. Coffey (2016). "EGF receptor ligands: recent advances." F1000Research **5**: F1000 Faculty Rev-2270.
Slater, C. R. (2017). "The Structure of Human Neuromuscular Junctions: Some Unanswered Molecular Questions." International journal of molecular sciences **18**(10): 2183.
Soleimani, V. D., V. G. Punch, Y.-i. Kawabe, A. E. Jones, G. A. Palidwor, C. J. Porter, J. W. Cross, J. J. Carvajal, C. E. M. Kockx, W. F. J. van Ijcken, T. J. Perkins, P. W. J. Rigby, F. Grosveld and M. A. Rudnicki (2012). "Transcriptional dominance of Pax7 in adult myogenesis is due to high-affinity recognition of homeodomain motifs." Developmental cell **22**(6): 1208-1220.
Southard, S., S. Low, L. Li, M. Rozo, T. Harvey, C.-M. Fan and C. Lepper (2014). "A series of Cre-ERT2 drivers for manipulation of the skeletal muscle lineage." genesis **52**(8): 759-770.
Su, N., J. Yang, Y. Xie, X. Du, H. Chen, H. Zhou and L. Chen (2019). "Bone function, dysfunction and its role in diseases including critical illness." International journal of biological sciences **15**(4): 776-787.
Taichman, R. S. (2005). "Blood and bone: two tissues whose fates are intertwined to create the hematopoietic stem-cell niche." Blood **105**(7): 2631-2639.
Tseng, W., J. Lu, G. A. Bishop, A. D. Watson, A. P. Sage, L. Demer and Y. Tintut (2010). "Regulation of interleukin-6 expression in osteoblasts by oxidized phospholipids." Journal of lipid research **51**(5): 1010-1016.
Vandenput, L., K. Sjögren, J. Svensson and C. Ohlsson (2012). "The role of IGF-1 for fracture risk in men." Frontiers in endocrinology **3**: 51-51.
Verghese, J., R. B. Lipton, M. J. Katz, C. B. Hall, C. A. Derby, G. Kuslansky, A. F. Ambrose, M. Sliwinski and H. Buschke (2003). "Leisure activities and the risk of dementia in the elderly." N Engl J Med **348**(25): 2508-2516.

Wannamethee, S. G., A. G. Shaper and K. G. Alberti (2000). "Physical activity, metabolic factors, and the incidence of coronary heart disease and type 2 diabetes." Arch Intern Med **160**(14): 2108-2116.

Welc, S. S. and T. L. Clanton (2013). "The regulation of interleukin-6 implicates skeletal muscle as an integrative stress sensor and endocrine organ." Experimental physiology **98**(2): 359-371.

Wu, Q., X. Zhou, D. Huang, Y. Ji and F. Kang (2017). "IL-6 Enhances Osteocyte-Mediated Osteoclastogenesis by Promoting JAK2 and RANKL Activity In Vitro." Cell Physiol Biochem **41**(4): 1360-1369.

Yamada, T. and H. Katagiri (2007). "Avenues of Communication between the Brain and Tissues/Organs Involved in Energy Homeostasis." Endocrine Journal **advpub**: 0705170024-0705170024.

Yao, Z., M.-H. Lafage-Proust, J. Plouët, S. Bloomfield, C. Alexandre and L. Vico (2004). "Increase of Both Angiogenesis and Bone Mass in Response to Exercise Depends on VEGF." Journal of Bone and Mineral Research **19**(9): 1471-1480.

Yoshitake, F., S. Itoh, H. Narita, K. Ishihara and S. Ebisu (2008). "Interleukin-6 directly inhibits osteoclast differentiation by suppressing receptor activator of NF-kappaB signaling pathways." J Biol Chem **283**(17): 11535-11540.

Zammit, P. S. (2017). "Function of the myogenic regulatory factors Myf5, MyoD, Myogenin and MRF4 in skeletal muscle, satellite cells and regenerative myogenesis." Seminars in Cell & Developmental Biology **72**: 19-32.

Zhang, S., X. Wang, G. Li, Y. Chong, J. Zhang, X. Guo, B. Li and Z. Bi (2017). "Osteoclast regulation of osteoblasts via RANK-RANKL reverse signal transduction in vitro." Molecular medicine reports **16**(4): 3994-4000.

Zhang, X., J. Tamasi, X. Lu, J. Zhu, H. Chen, X. Tian, T.-C. Lee, D. W. Threadgill, B. E. Kream, Y. Kang, N. C. Partridge and L. Qin (2011). "Epidermal growth factor receptor plays an anabolic role in bone metabolism in vivo." Journal of bone and mineral research : the official journal of the American Society for Bone and Mineral Research **26**(5): 1022-1034.

Zurlo, F., K. Larson, C. Bogardus and E. Ravussin (1990). "Skeletal muscle metabolism is a major determinant of resting energy expenditure." J Clin Invest **86**(5): 1423-1427.

Appendix

Figure S1 to S3 were extracted from:

Myf6/MRF4 is a Myogenic Niche Regulator Required for the Maintenance of the Muscle Stem Cell Pool. Felicia Lazure, Darren M. Blackburn, **Nabila Karam,** Korin Sahinyan, Ahmad Sharanek, Duy Nguyen, Aldo H. Corchado, Christoph Lepper, Hamed S. Najafabadi, Theodore J. Perkins, Arezu Jahani-Asl, Vahab Soleimani. bioRxiv 691386.

With the permission of my supervisor Dr. Vahab Soleimani and my co-authors.

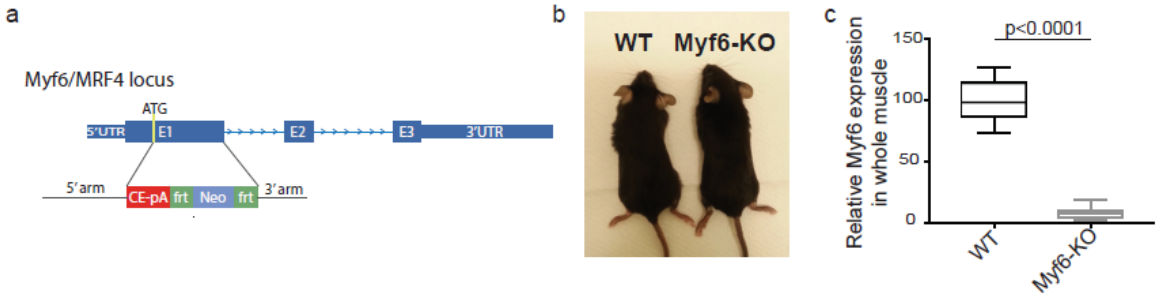

Figure S1: **(a)** Schematic drawing of the *Myf6* locus showing insertion of Cre-ER^{T2} sequence rendering the *Myf6* locus as a null allele. **(b)** Picture of 8 week-old *Myf6*-KO and WT mice. **(c)** Relative expression of Myf6 transcript in the hindlimb skeletal muscles of *Myf6*-KO and WT mice measured by Quantitative Real-Time PCR (RT-qPCR).

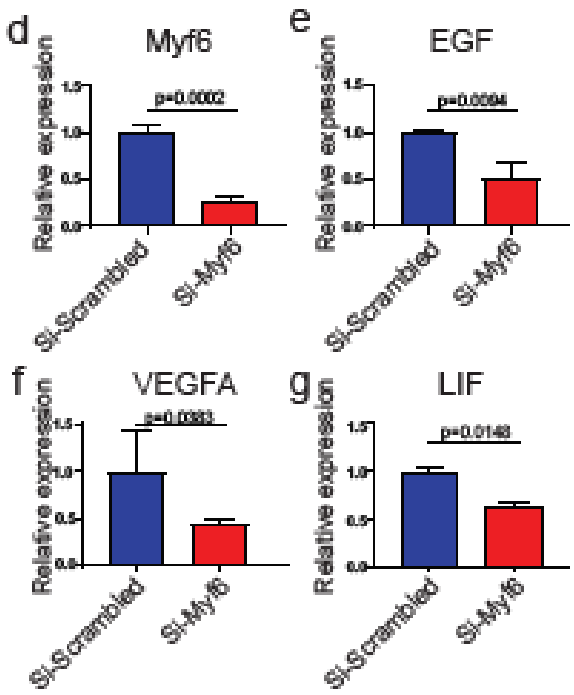

Figure S2: Depletion of *Myf6* transcript by siRNAs in differentiated primary myotubes (5DM). **(e-g)** Depletion of Myf6 expression by siRNAs leads to a significant reduction in the gene expression output of Epidermal Growth Factor (EGF) **(e)**, Vascular Endothelial Growth Factor A (VEGFA) **(f)** and Leukemia Inhibitory Factor (LIF) **(g).**

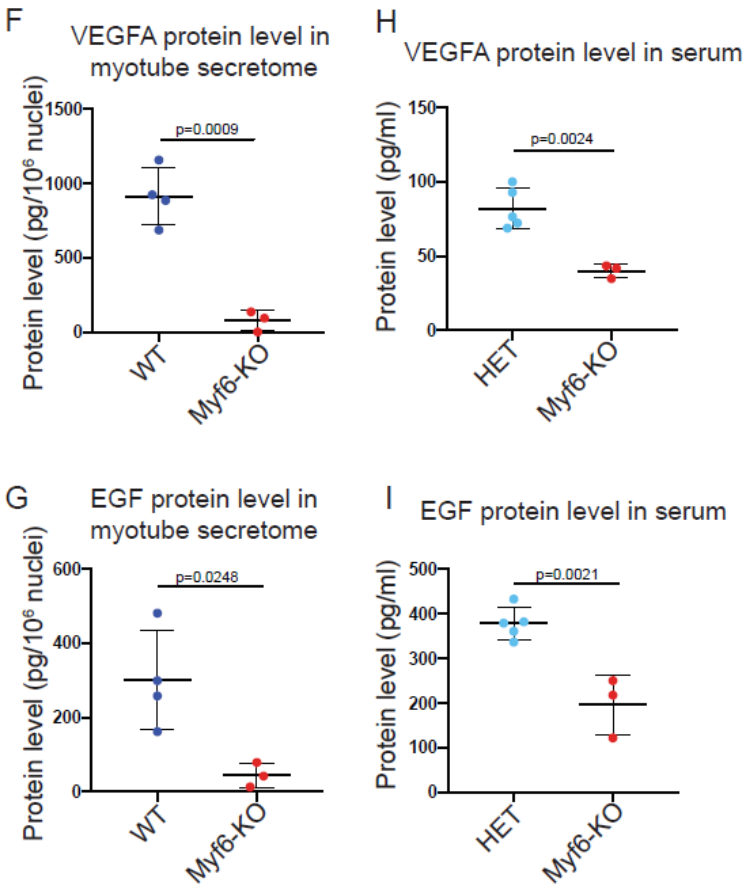

Figure S3: **(f)** VEGFA protein level in the secretome and **(g)** EGF in the secretome. **(h)** VEGFA proteins level in the blood serum, and **(i)** EGF protein level in blood serum. All were measured by Enzyme-Linked Immunosorbent Assay (ELISA).

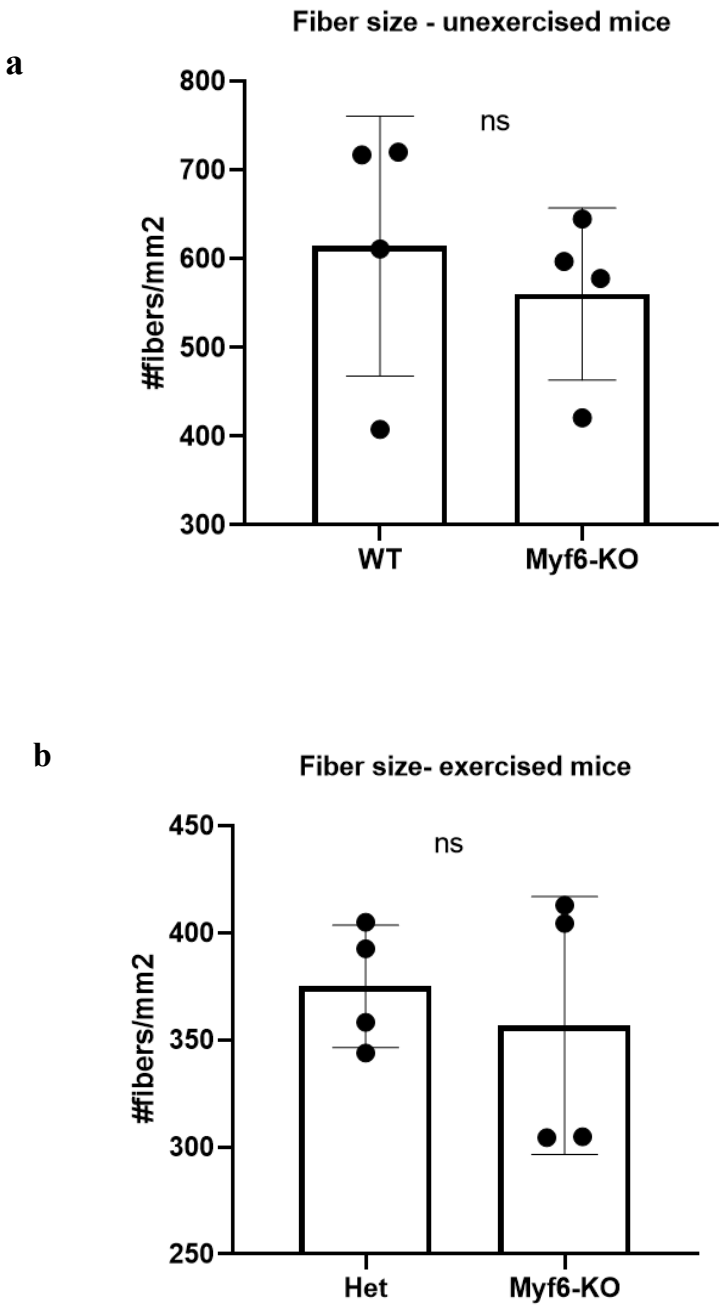

Figure S4: Muscle fiber size. **a.** Fiber size of unexercised mice (steady state). **b.** Fiber size of exercised mice (after the swimming test), N=4, 5 months old. The size is expressed as number of fibers present in every 1mm^2 of the cross-sections. Note that the greater the number of fibers, the smaller they are. N= 4 biological replicates.

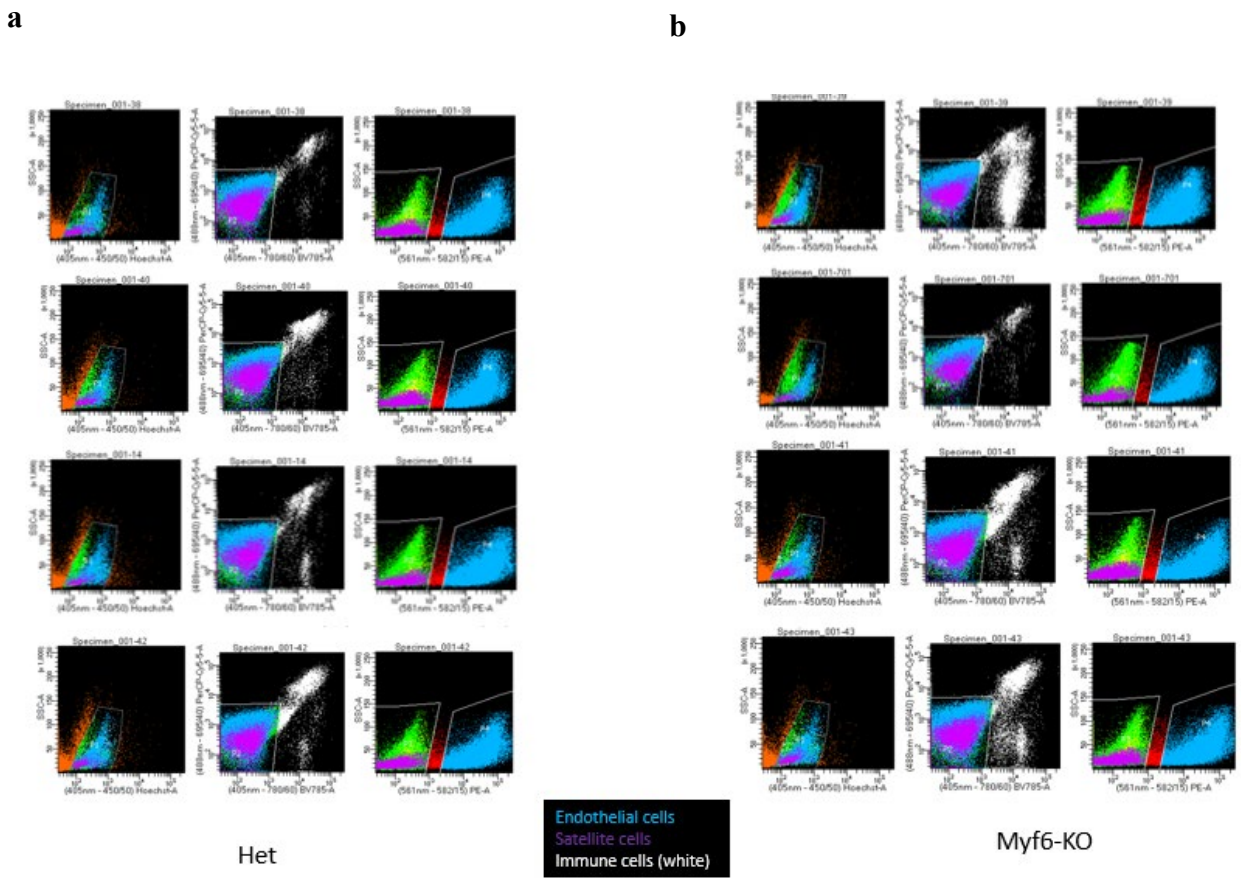

Figure S5: Fluorescence activated cell sorting (FACS) plots of hindlimb muscle for each mouse. Blue dots are endothelial cells, purple dots are satellite cells, white dots are immune cells (not gated in this case). **a.** FACS plots for the hindlimb of heterozygous mice (control). **b.** FACS plots for the hindlimb of the *Myf6*-KO mice. N=4 biological replicates.

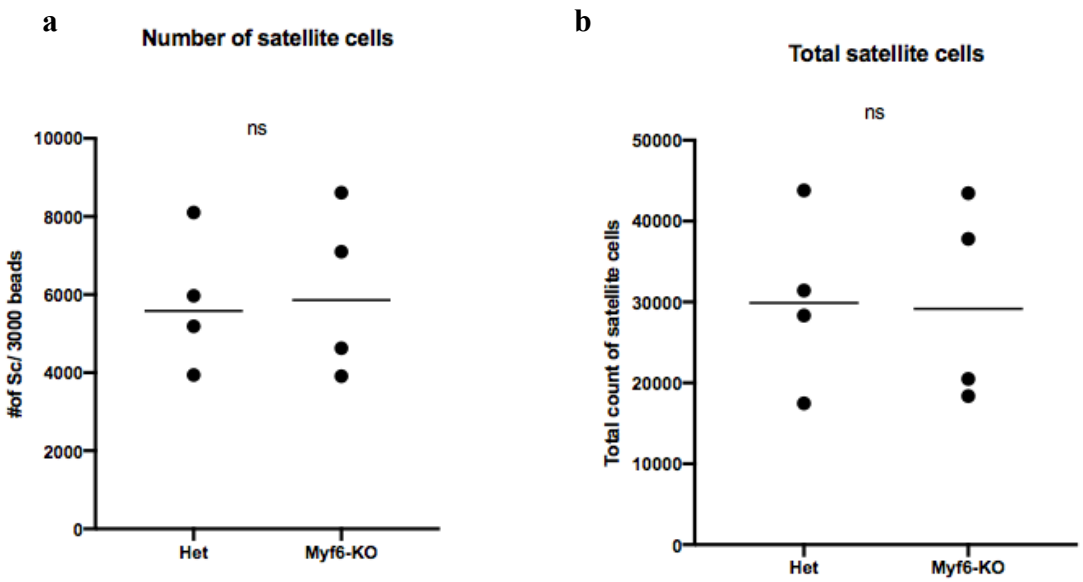

Figure S6: Quantification of satellite cells in the hindlimb muscle for the heterozygous (control) and *Myf6*-KO mice. **a.** Number of satellite cells per 3000 beads. **b.** Total satellite cells per mouse, for the same mass of lean hindlimb muscle. N= 4 biological replicates.

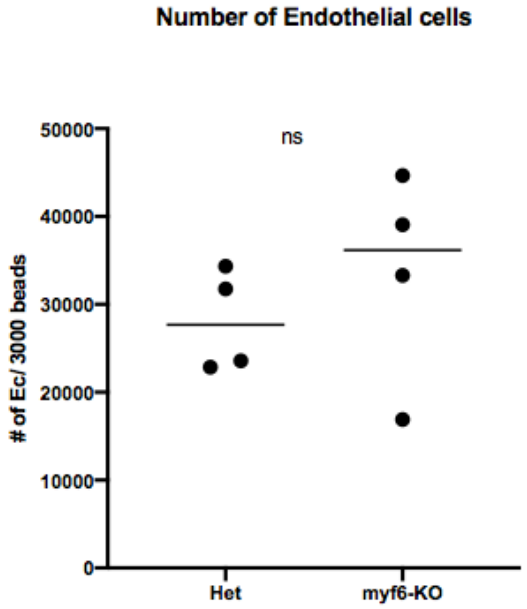

Figure S7: **Quantification of endothelial cells in the hindlimb muscle for the heterozygous (control) and *Myf6*-KO mice**. Number of satellite cells per 3000 beads. N=4 biological replicates.

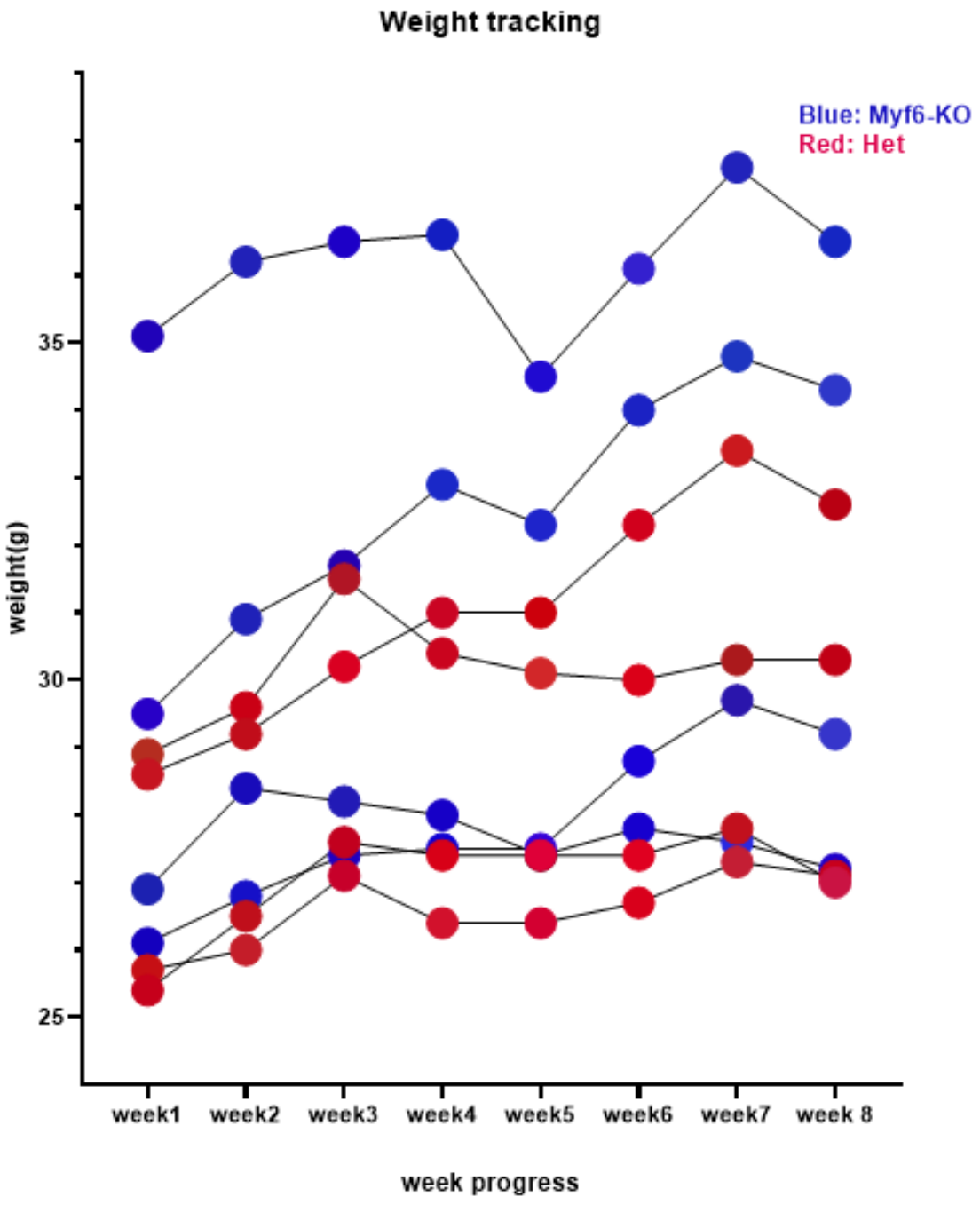

Figure S8: Weight tracking of the swimming mice. Starting from the end of conditioning, up to the last week of the program (week 8). Blue dots represent *Myf6*-KO mice, red dots are for the heterozygous mice (control).

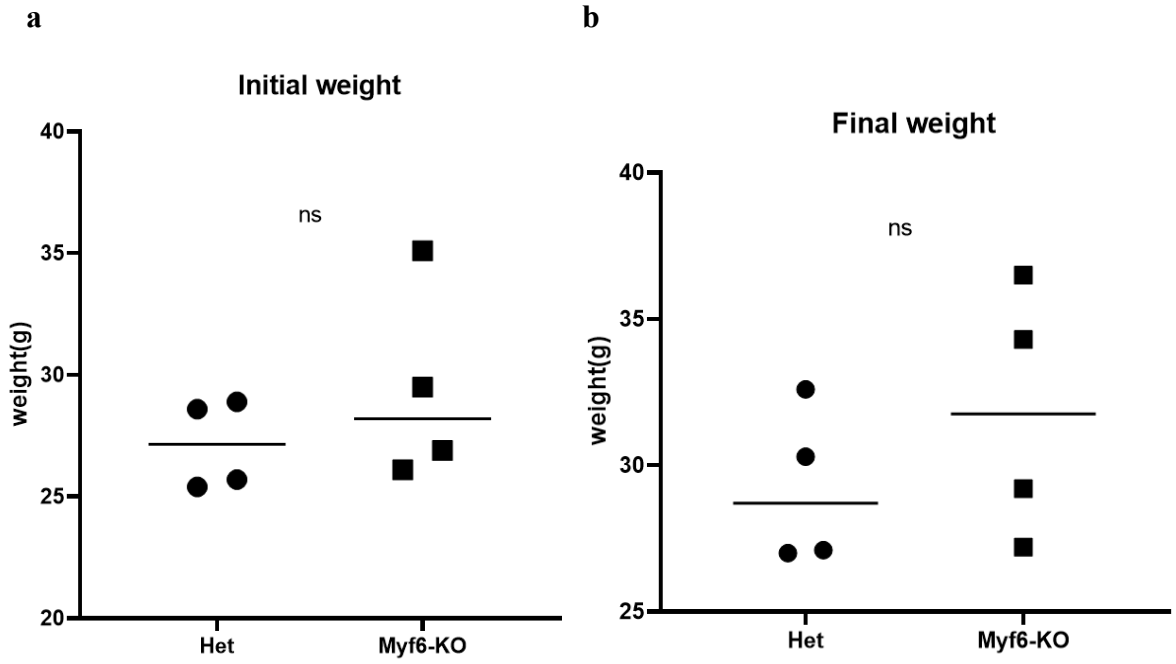

Figure S9. Comparison of the swimming mice weight.a. After conditioning and **b.** at the end of the swimming program. N= 4 biological replicates.

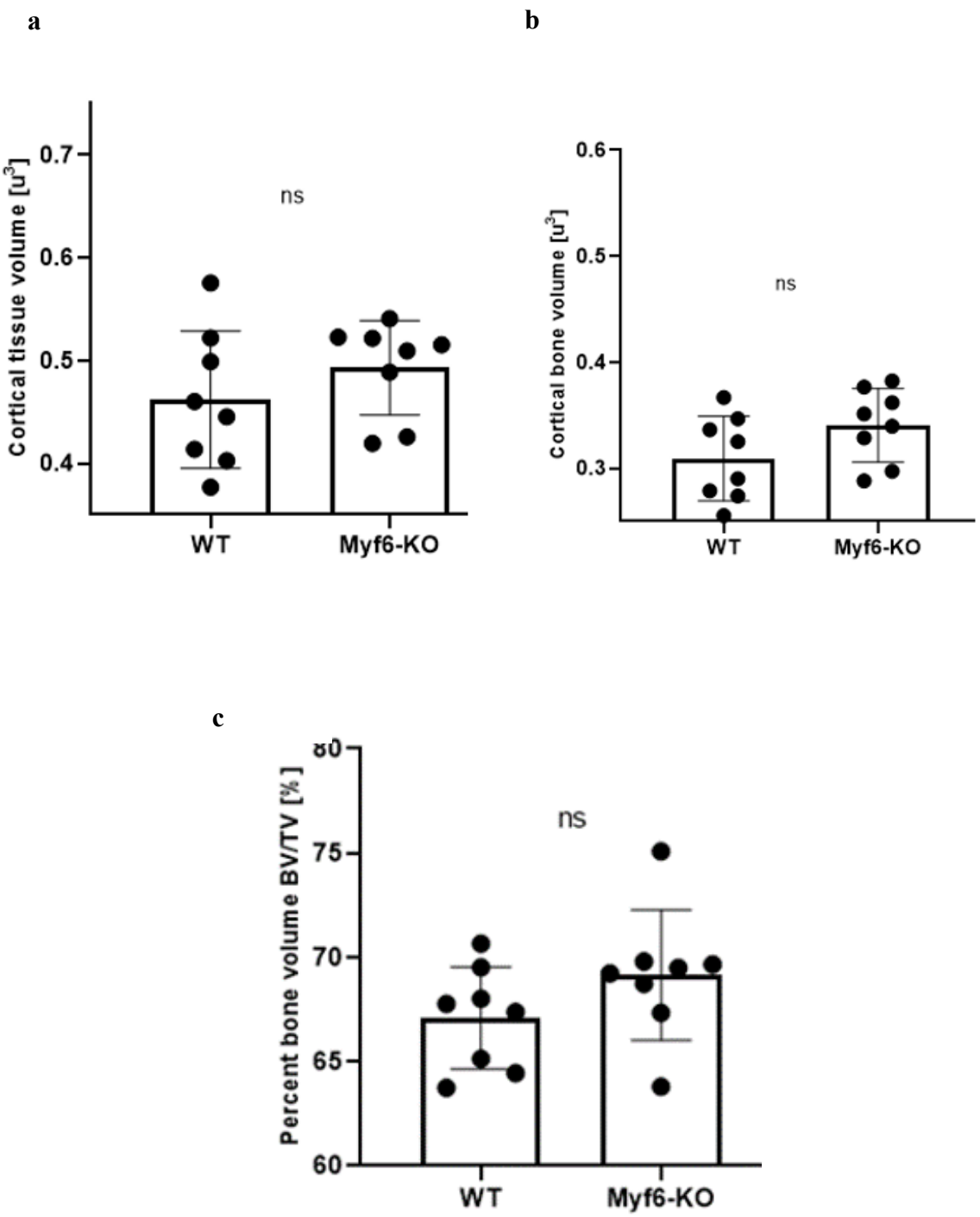

Figure S10: Cortical bone volume analysis of the tibia at steady state. Raw microCT data measuring the volumetric parameters of the cortical bone. **a.** Cortical tissue volume (mm^3). **b.** Cortical bone volume (mm^3). **c.** Percent bone volume BV/TV (%). N= 8 biological replicates.

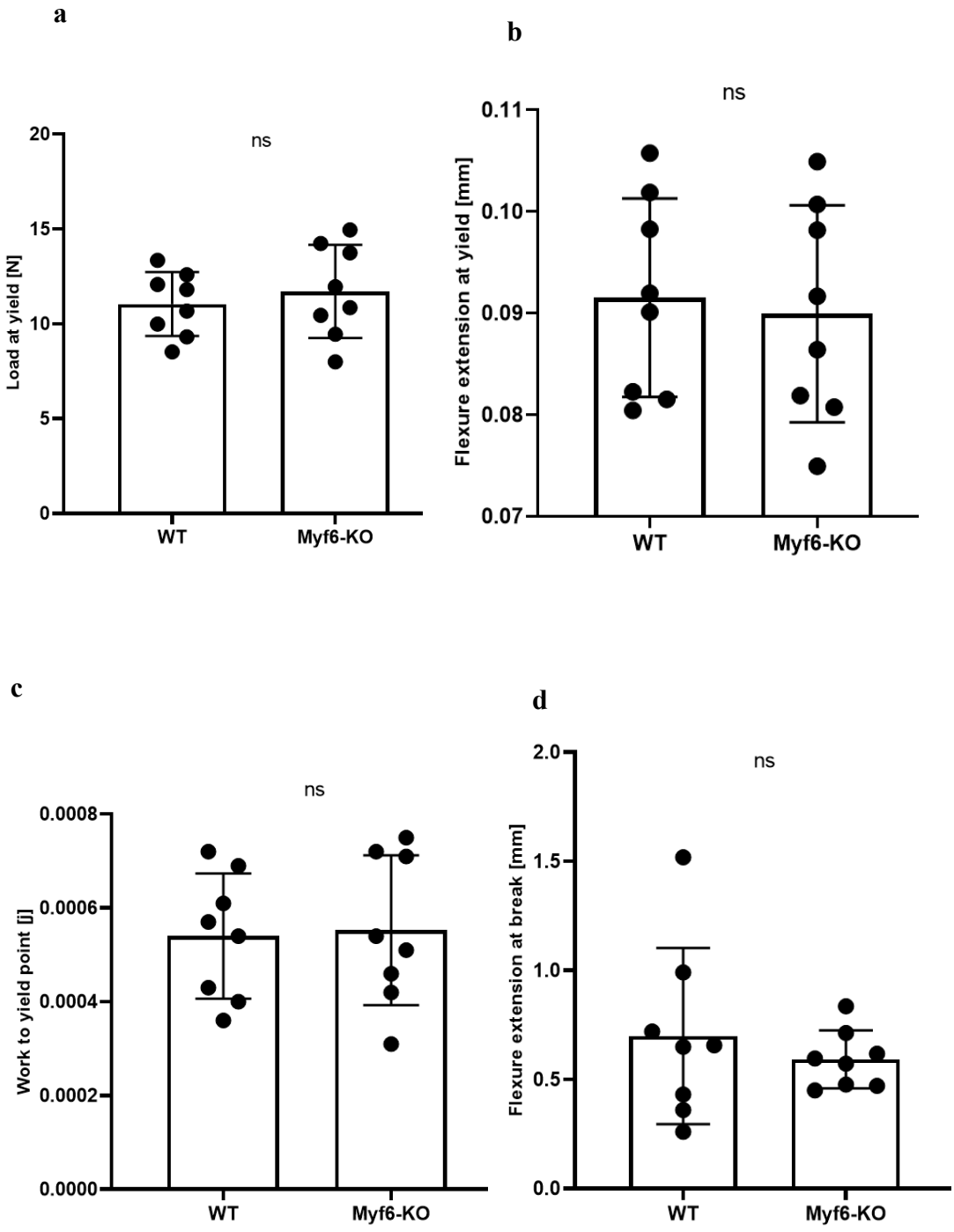

Figure S11: Three-point bending tests results of the steady-state cohort. a. Load at yield (N). **b**. Flexure extension at yield (mm). **c.** work to yield point (j). **d.** Flexure extension at break (j). N= 8 biological replicates.

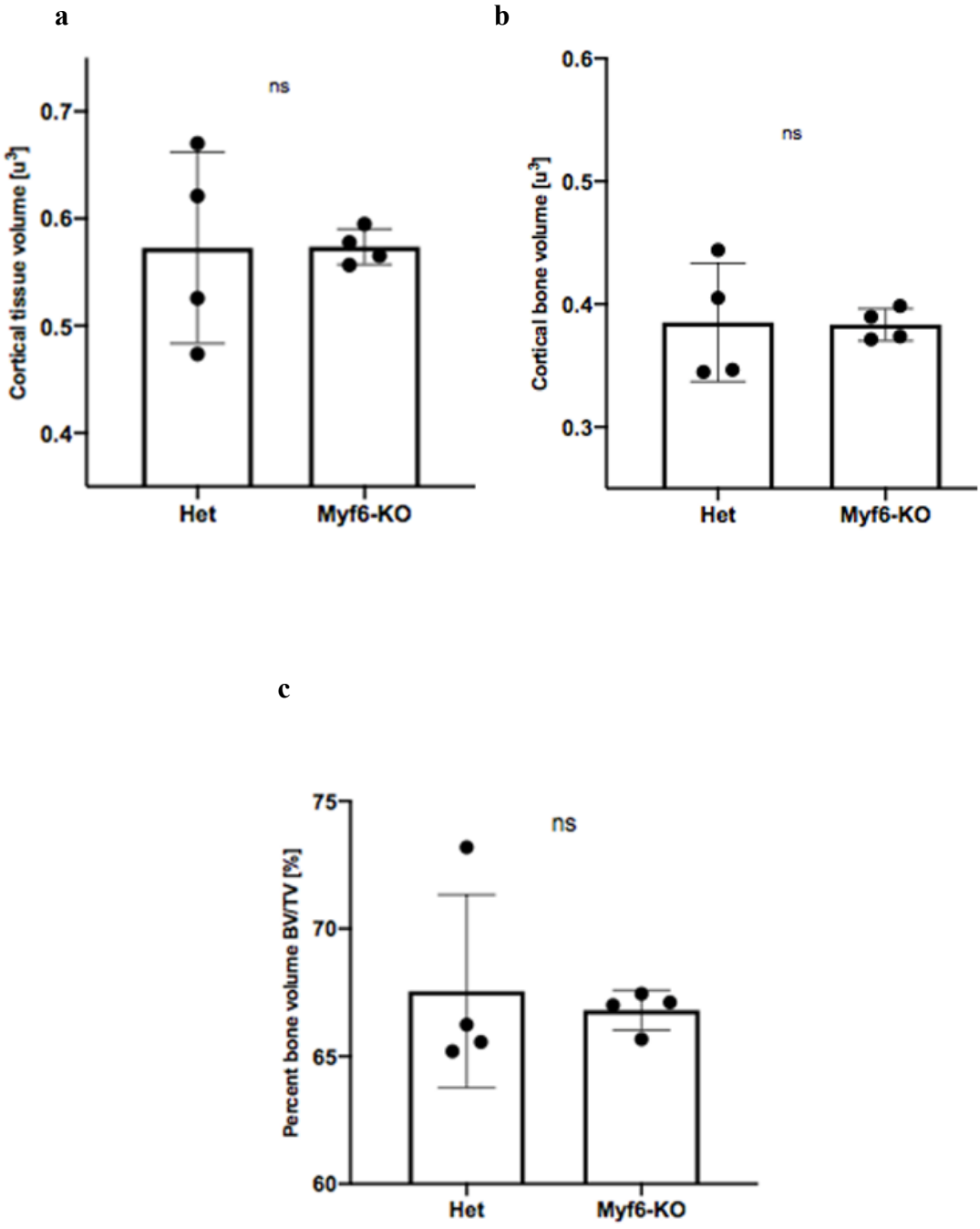

Figure S12: Cortical bone analysis of the tibia at active state. Raw microCT data measuring the volumetric parameters of the cortical bone. **a.** Cortical tissue volume (mm^3). **b.** Cortical bone volume (mm^3). **c.** Percent bone volume BV/TV (%). N=4 biological replicates.

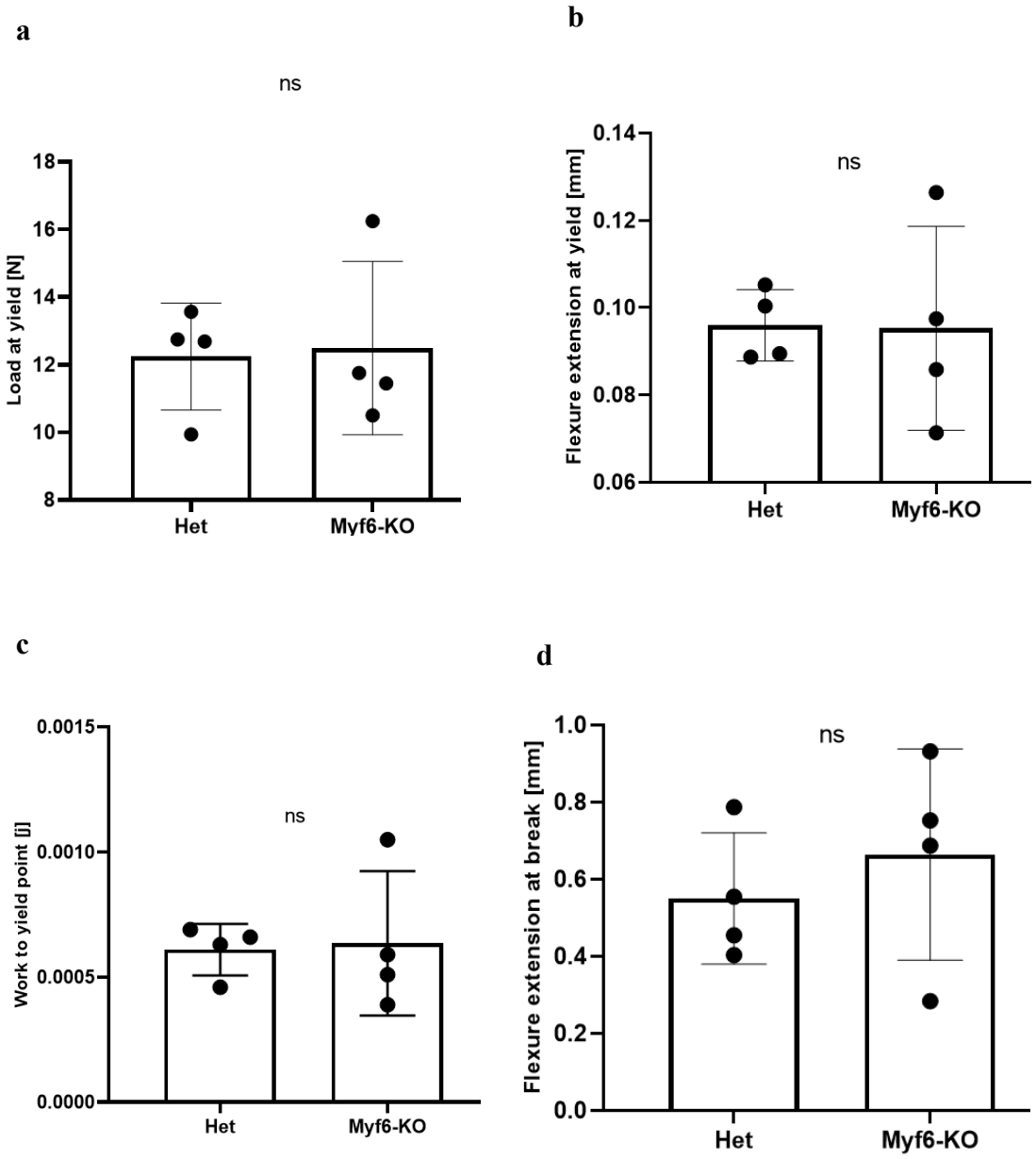

Figure S13: Three-point bending tests results of the active cohort. a. Load at yield (N). **b**. Flexure extension at yield (mm). **c.** work to yield point (j). **d.** Flexure extension at break (j). N=4 biological replicates.

McGill

July 23, 2019

Animal Certificate

This is to certify that **Dr. Vahab Soleimani, Department of Human Genetics, Lady Davis Institute,** currently holds an approved Animal Use Protocol **# 2014-7512** with McGill University and its Affiliated Hospitals' Research Institutes for the following project:

Animal Use Protocol Title: Molecular regulation of skeletal muscle regeneration

Start date: July 1, 2019

Expiration date: July 1, 2020

McGill University and Affiliated Hospitals Research Institutes recognize the importance of animal research in our efforts to further our knowledge of natural processes, diseases and conservation. Research, educational and testing projects are conducted with full commitment to the wellbeing of the animal subjects. In order to limit animal use to meritorious research or educational projects, the institution relies on stringent peer review processes, along with assessment of ethical issues by the Animal Care Committee. McGill University recognizes that the use of animals in research, teaching and testing carries significant responsibilities. The institution will continue to develop and maintain guidelines and regulations, following the high standards established by the Canadian Council on Animal Care. It is committed to conducting the highest-quality research and to providing animals with the best care.

Melanie Tremblay, Ph.D
Animal Ethics and Compliance Admin | Animal Compliance Office
Office of Vice-Principal (Research and Innovation)
Suite 325, James Administration Building, McGill University
845 Sherbrooke Street West, Montreal, Quebec, Canada H3A 0G4
animal.approvals@mcgill.ca